Mineralogy of some Ag-(Cu)-Pb-Bi sulphide associations

SVEN KARUP-MØLLER

Karup-Møller, S.: Mineralogy of some Ag-(Cu)-Pb-Bi sulphide associations. *Bull. geol. Soc. Denmark*, vol. 26, pp. 41–68, Copenhagen, August 1st 1977. https://doi.org/10.37570/bgsd-1976-26-03

Microprobe analyses and x-ray crystallographic studies have resulted in the discovery of the following new minerals: vikingite ($Ag_{1.00}Pb_{2.50}Bi_{3.00}S_{7.5}$, Z = 4, a = 13.603(6)Å, b = 25.248(7)Å, c = 4.112(4)Å, γ = 95.55(3)°, space group: B2/m or Bm), eskimoite ($Ag_{1.50}Pb_{3.00}Bi_{3.50}S_9$, Z = 4, a = 13.459(5)Å, b = 30.194(8)Å, c = 4.100(5)Å, γ = 93.35(5)°, space group: B2/m or Bm), ourayite ($Ag_{12.5}Pb_{15}Bi_{20.5}S_{52}$, Z = 1, a = 13.457(14)Å, b = 44.042(40)Å, c = 4.100(10)Å, space group: Bbmm or Bb2$_1$m) and treasurite ($Ag_{1.75}Pb_{1.50}Bi_{3.75}S_8$, Z = 4, a = 13.349(10)Å, b = 26.538(20)Å, c = 4.092(7), γ = 92.77(7)°, space group: B2/m, B2 or Bm). Several related mineral varieties are partly described. Their compositions have been determined but they are present in insufficient amounts for x-ray crystallographic examinations. They have not been given names. Microprobe analyses are given for associated minerals: members of the lillianite-gustavite solid solution series, heyrovskyite, galena, galenobismutite, members of the bismuthinite-aikinite series and berryite. Crystallization sequences and temperatures of formations are described and discussed. The new mineral species, the unnamed mineral varieties, the members of the lillianite-gustavite solid solution series and heyrovskyite belong to the "lillianite homologous series" (*LHS*).

S. Karup-Møller, Mineralogical Institute, Technical University of Denmark, 2800 Lyngby, Denmark.
January 25th, 1977.

Table of Contents

Ag-Cu-Pb-Bi sulphide assemblages from world-wide deposits have been studied. Sizable amounts of material were obtained from the cryolite deposit at Ivigtut in Greenland. Other parageneses examined were contained in rare museum specimens borrowed from different institutions. Several new mineral species were discovered which allowed the development of a chemical and crystallographic classification of the lillianite homologous series (LHS). The details are given in Makovicky and Karup-Møller (1977a, b). New compositional data were obtained for the associated minerals pavonite, benjaminite, berryite, cosalite, galenobismutite, members of the bismuthinite-aikinite series and Ag-Bi-bearing galena.

Four new minerals, vikingite, eskimoite, ourayite and treasurite, were submitted to the Commission on New Minerals and Mineral Names (IMA) jointly by the author and E. Makovicky, University of Copenhagen, and were approved in April, 1976.

Chemical-Structural Classification of the Lillianite Homologues

The compositional field of the LHS is bound by the tie lines galena-galenobismutite, galenobismutite-matildite and matildite-galena (fig. 1). The galena-matildite solid solution series may be considered a limiting case of the LHS. Pavonite and benjaminite posess a closely related structural motif (Karup-Møller & Makovicky 1977). Galenobismutite does not belong to the series.

The crystal structure of lillianite homologues consist of layers with 'galena-like structure' parallel to (010) and separated by discontinous layers of Pb atoms in trigonal prismatic coordination (fig. 2). The basic difference among distinct members of the lillianite homologous series is the thickness of the galena-like layer. Each layer consists of chains, parallel to h or h′ (fig. 2), composed of integer number N of octahedra. The chains extend in a zig-zag fashion throughout the structure of the mineral.

Basically we may distinguish between lillianite homologues in which all the galena-like layers have the same thickness ($N_1 = N_2$, resulting in

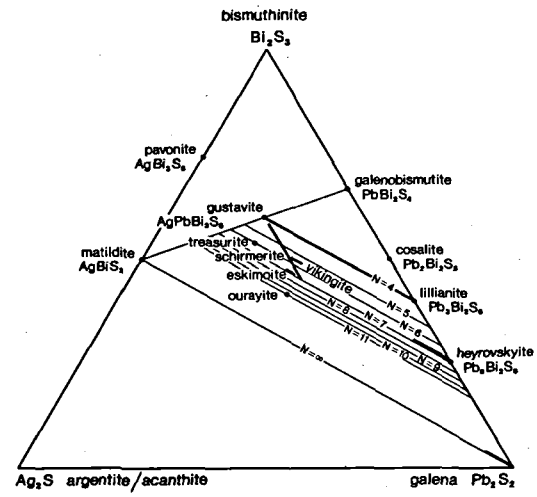

Fig. 1. Diagram showing all fully described Ag-Pb-Bi sulphides. The lillianite homologous series plots within the triangle bound by galena, matildite and galenobismutite. The position is shown of each structural member characterized by the integer N values ranging from 4 to 11. (For structural meaning of N, see text). The individual lillianite homologues are plotted on their N lines. The compositional range of schirmerite, vikingite, eskimoite and heyrovskyite is shown in heavy lines. Numerous members of the lillianite-gustavite series (N= 4) have been identified, which is also indicated by a heavy line. Cosalite plots within the triangle but it is not a true lillianite homologue.

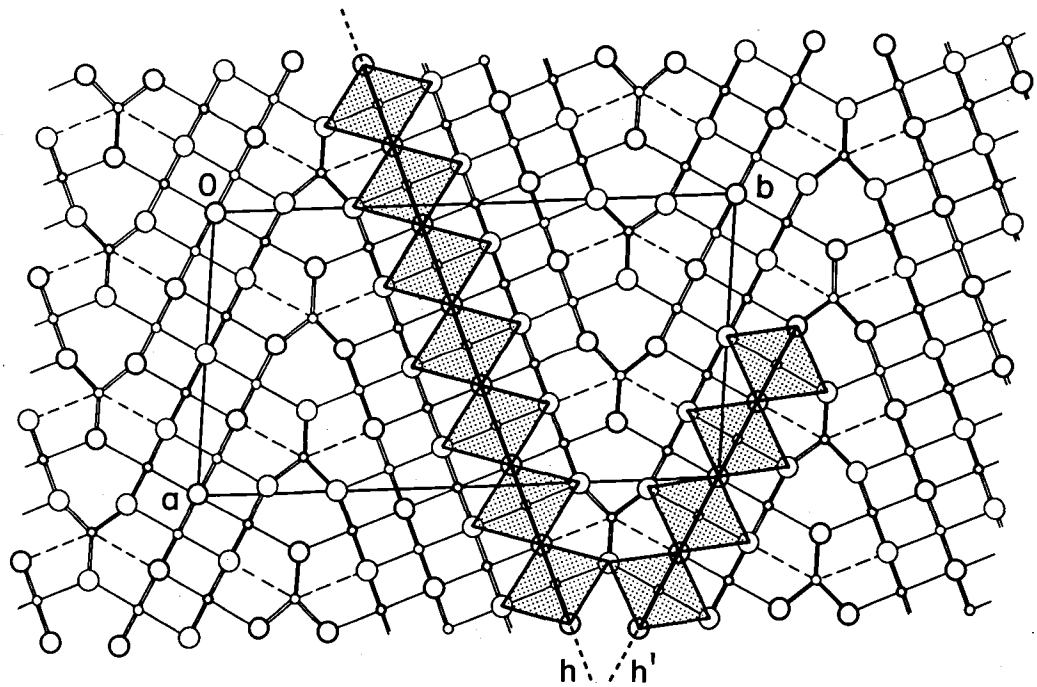

Fig. 2. Idealized structure of vikingite projected on (001). The unit cell is traced. h: chain of 7 octahedra and h': chain of 4 octahedra characterizing the vikingite N_1–N_2 combination. Large circles: sulphur atoms and small circles: metal atoms.

an orthorhombic structure) and the lillianite homologues in which the N-values of adjacent layers are different ($N_1 \neq N_2$, and the structure is monoclinic, e.g. fig. 2).

At present the following fully described natural minerals (with N_1–N_2 combinations in brackets) are known: gustavite-lillianite (4–4), vikingite (4–7, fig. 2), eskimoite (5–9), ourayite (11–11), treasurite (4–8) and heyrovskyite (7–7). Members with average N ($= \frac{N_1+N_2}{2}$) less than 4 have not been found in nature.

The following formulae represent any member of the lillianite homologous series with silver absent (1) and silver present (2). (T: trigonal prismatic coordinated and O: octahedrally coordinated metals):

(1) $Pb^{T}Pb^{O}_{N-2}\,Bi_2^{O}S_{N+2}$ (Z = 4)

(2) $Pb^{T}Pb^{O}_{(N-2)-2x}\,Bi^{O}_{2+x}\,Ag_x^{O}S_{N+2}$
(Z = 4, $x_{max} = \frac{N-2}{2}$ assuming
Ag + Bi ⇆ 2 Pb)

All the Ag-free members of the series plot on the join galena-galenobismutite. The fully substituted members on any given N-line, i.e. those with maximum silver, plot on the line between galenobismutite and matildite (fig. 1). Thus in principle any ideal lillianite homologue can be characterized by its N and x values. The latter is termed 'the substitution factor'.

The values for N and x can be calculated on the basis of:

(3) Me/S
(4) Ag/Pb/Bi

From (3), x can be calculated for each element in (2) and the difference between x (max) and x (min), termed Δx, expresses the accuracy for the microprobe analyses. Similarly, if N calculated from (4) is applied to sulphur, the resulting formula again will yield a Δx value showing the goodness of fit of the calculated x and N values to the entire chemical analysis. (For the calculation details see Makovicky & Karup-Møller 1977a).

The x-value of a mineral plotting on one N line cannot be directly compared with the x value representing a mineral plotting on another N li-

ne. In order to make the substitutions comparable, the 'substitution percentage' (L %) has been introduced. This value is 100 % for fully substituted Ag-Bi-end members, and 0 % for those lying on the galena-galenobismutite join. In tables 1 and 2, with microprobe analyses for members of the lillianite homologous series, the values N, L, x and Δx have been computed on the basis of (3) and (4) above.

The values computed using ratio (3) are extremely sensitive to the accuracy of the sulphur determinations. In general, the determination of this element is less accurate than those obtained for the metals. The values computed on the basis of (3) may therefore be used preferably as a control on the accuracy of the sulphur determinations provided that the metal determinations are reasonably correct.

The formulae for all lillianite homologues based on: 'sum of metals = Crystallographic (ideal) N + 1' can be read directly from tables 1 and 2. The formulae and the values for N, L %, x and Δx (four last columns in tables 1 and 2), given in the mineral description section page 45 to 57, are based on the 'Ag/Pb/Bi' ratio.

From the above it is seen that any lillianite homologue can be characterized unambiguously by its N (average) and L % values. The expression $^{4.0}L_{69.7}$ would thus characterize a member of the series with N = 4.0 and a substitution persentage equal to 69.7. If one or both end members of a series with a certain N value are known, for example the lillianite-gustavite series, the intermediate member may be characterized as $^{4.0}Gus_{35.6}Lil_{64.4}$ or more briefly as either $^{4.0}Gus_{35.6}$ or $^{4.0}Lil_{64.4}$. This corresponds to the feldspar notation $An_{35.6}Ab_{64.4}$.

N lines up to N = 11 are plotted in fig. 1. Minerals with N greater than 11 have not yet been discovered. With increasing N the distance between the lines decreases and it becomes increasingly difficult to determine the correct N values exclusively on the basis of the chemical analyses. Single crystal studies must be carried out.

The thickness of a galena-like layer in the structure of a lillianite homologue may be subject to structural errors. The average N value of a mineral determined by chemical analyses may therefore be somewhat different from the ideal crystallographic N value. This feature is recognized as continuous streaks, parallel to b*, in the Weissenberg photographs and as tails of otherwise sharp reflections parallel to b*.

Metal vacancies might occur in the structure of a mineral due to the substitution of $3Pb^{++}$ by $2Bi^{+++}$ (Otto & Strunz 1968). One lead position would thus be left empty. As a result of this, microprobe analyses will again yield slightly altered N values, which will always be less than the ideal N.

Copper, in amounts up to half a weight percent, occurs in several of the minerals. It is assumed that the metal occurs in the tetrahedral vacancies. Due to the small amounts of copper, the results of the calculations based on the pure 'Ag+Bi→2Pb' substitution are only slightly altered. The calculations in tables 1 and 2 are therefore based upon the Ag/Pb/Bi ratio ignoring the presence of copper.

Materials Studied

Only the sulphides related to the system Ag-(Cu)-Pb-Bi-S are described. Several of the specimens were investigated previously (Karup-Møller 1966, 1970, 1972, 1973a, 1973b) and have been re-investigated in the present study. Crystal-chemical details are given in Makovicky & Karup-Møller (1977a, 1977b) and Karup-Møller & Makovicky (in prep). The following abbreviations are used for these references: KM66, KM70, KM72, KM73a, KM73b, M-KM77a, M-KM77b and KM-M77. The institutions where the specimens are kept are given in brackets. These are: Geological Museum, University of Copenhagen (GMC), Royal Ontario Museum, Canada (ROM) and University of Pennsylvania, USA (UP).

1. Gustavite-cosalite-galena mineral specimens from Ivigtut, South Greenland. Gustavite, vikingite, eskimoite, berryite, aikinite, mineral A and galena (KM66, KM70, KM72, KM73a and M-KM77. GMC).
2. Specimen 1139. Old Lout Mine, Ouray, Colorado, USA. Bismuthinite, pavonite, benjaminite, gustavite, $^{5.90}L_{65.7}$ and galena. (KM72. UP).
3. Polished sections 2568 and 2569. Kingsgate, Australia. Bismuthinite, cosalite, galenobismutite, $^{3.75}Gus_{40.2}$ and galena (GMC).
4. Polished sections 2953 and 2954. Agenosawa Mine, Japan. Bismuthinite, cosalite, $^{3.85}Gus_{51.0}$, $^{3.89}Gus_{29.1}$ and galena. (GMC).

5. Polished sections LS70-B4-1 and -2. Is Lassinus, Sardinia, Italy. $^{3.66}Gus_{55.8}$, cosalite, hammarite and galena (University Vrije, Amsterdam, Holland).
6. Polished section 2801. Yakuki Mine, Fukushima Pref., Japan. $^{3.86}Gus_{21.2}$ and $^{6.68}Hey_{9.6}$. (GMC).
7. Specimen 1124. Alaska Mine, Colorado, USA. Pavonite, "cupro-pavonite" and gustavite. (KM72 and KM-M77.UP).
8. Specimen 1140. Gladiator Mine, Colorado, USA. Bismuthinite, pavonite, gustavite, aikinite and galena. (KM72.UP).
9. Specimen BSF 1821. Silver Bell Mine, Red Mountain, Colorado, USA. Pavonite, bismuthinite and gustavite. (KM72 and KM-M77). (Mining school, Filipstad, Sweden).
10. Specimen ROM M21003. Bolivar mine, Cerro Bonete, Lipez Province, Bolivia. Pavonite (?), Bismuthinite and krupkaite (?). (KM72 and KM-M77. ROM).
11. Specimen ROM M13805. Manhattan, Nevada, USA. Benjaminite-gustavite (a submicroscopic intergrowth), berryite, and krupkaite (?). (KM72 and KM-M77. ROM).
12. PS.2550. McElroy Township, Ontario, Canada. Cosalite and krupkaite (?). (GMC).
13. Polished section 2571. Treasury mine, Colorado, USA. Schirmerite and a schirmerite decomposition mineral. (Ramdohr 1960, KM 73b and M-KM77b. University of Heidelberg, Germany).
14. Specimen R9714. Treasury Lodge, Geneva district, Colorado, USA. Treasurite and treasurite decomposition mineral. (KM73b and M-KM77. Smithsonian Institution, Washington, USA).
15. Specimen ROM M4100. Old Lout Mine, Ouray, Colorado, USA: Ourayite, galena and matildite. (KM73b and M-KM77. ROM).

Mineral Descriptions

The identification of all the minerals described in this chapter is based upon microprobe analyses and in several cases also upon Weissenberg single crystal studies.

The optical properties of copper-free lillianite homologues are so similar that distinction between them is not possible, not even when observed in mutual contact.

The x-ray powder patterns of many of the minerals are of poor quality, especially when the Guinier technique is used. This feature, and the close structural relationships resulting in similar powder patterns among the minerals, practically excludes positive identification from powder patterns. The powder patterns representing the four new minerals, vikingite, eskimoite, treasurite and ourayite, have been optained using fragments mounted in the Gandolfi camera after having been investigated by the Weissenberg method.

Microprobe data for lillianite homologues analyzed by the author are listed in table 1 and plotted in figs 3–6. Published analyses of known members of the lillianite homologous series are listed in table 2 and plotted in fig. 7. In the plots copper is assumed to have substituted for silver and antimony for bismuth. The atomic ratios in the two tables are based upon the formula (2). The analysis numbers (first column in tables 1 and 2) correspond to those in figs 3 to 7. In the following, the reference, for instance, "table 1, 7" refers to analysis no. 7 in table 1, and the reference "fig. 3, 7" refers to analysis no. 7 in fig. 3.

The microprobe analyses of associated pavonite and benjaminite (table 1, A-K in KM-M77) are plotted in figs 5 and 6 (A-K).

Cosalite does not belong to the LHS. Analyses of cosalite (table 8, C1–C9) are plotted in figs 3 and 4, using the same reference numbers as in the table.

A Hitachi model XMB-5S microprobe was used during the present investigation (Mineralogical Institute, University of Copenhagen, Denmark). Standards were pure Ag, Cu, Bi, Sb and natural galena. The radiation lines were AgLα, CuKα, BiLα, SbLα, PbLα, and SKα. Corrections were made according to a modified programme after Springer (1977). The notation 'esd' in tables 1 and 7–11 stands for 'estimated standard deviation' and describes the spread of analyses completed on a suite of mineral grains with standard measurements taken before and after each sequence.

Vikingite

This mineral is known only from the Ivigtut gustavite-cosalite-galena paragenesis. It has been named after the early settlers of Greenland, the Vikings.

Vikingite is lamellar and has an average grain size of 0.5 mm. Reflectance pleochroism is absent in the air, absent to weak in oil. The reflectance colour is very similar to that of galena. Reflectance values recorded in air at the four principal wave lengths are according to Vendrell-Saz, Karup-Møller & Lopez-Soler (in press.): 481 (λ nm) = 44.6–45.4, 546 (λ nm) = 43.1–43.8, 589 (λ nm) = 42.5–43.2 and 644 (λ nm) = 42.1–42.8. Anisotropism by crossed nicols is distinct to strong. Anisotropism colours are light grey to steel bluish-black. Microindentation hardness ranges from 153–207 and averages 185±16 (20 grains measured, VHN_{50gr}).

TABLE 1. MICROPROBE ANALYSES ON MEMBERS OF THE LILLIANITE HOMOLOGOUS SERIES COMPLETED DURING THE PRESENT STUDY.

Analysis No.	POLISHED SECTION NUMBER, LOCALITY, MINERAL NAME AND SAMPLE DESCRIPTION	No grains analyzed	WT.% AND ESD. Ag	Cu	Pb	Bi	Sb	S	SUM	UNIT CELL FORMULA (Z=4) BASED ON SUM OF METALS(~Cu)=$N_{Cryst}+1$ Ag	Cu	Pb	Bi	Sb	S	N (Cryst.)
	Vikingite.															
1	41. Ivigtut.	8	8.2 0.2	0.2 0.1	30.4 0.5	46.2 0.7	- -	16.5 0.2	101.5	1.11	0.05	2.15	3.24	-	7.54	5.5
2	41. Ivigtut. 8 spots analyzed in one grain.	8	8.5 0.2	0.2 0.1	29.0 0.9	45.9 0.7	-	16.5 0.2	100.1	1.17	0.05	2.08	3.26	-	7.63	5.5
3	2. Ivigtut.	6	7.9 0.2	0.2 0.1	30.7 0.6	46.8 0.7	-	16.5 0.2	102.1	1.07	0.05	2.16	3.27	-	7.51	5.5
4	31. Ivigtut. Vikingite in galena matrix.	9	8.9 0.3	0.2 0.1	27.7 1.0	47.6 0.8	-	16.5 0.2	100.9	1.21	0.05	1.96	3.33	-	7.53	5.5
5	31. Ivigtut. Vikingite around galena areas.	10	8.9 0.3	0.2 0.1	28.0 1.4	47.3 1.0	-	16.5 0.2	101.0	1.21	0.05	1.98	3.31	-	7.53	5.5
	Eskimoite.															
6	35. Ivigtut.	15	9.7 0.4	0.3 0.1	28.8 0.9	46.7 1.1	-	16.2 0.4	101.7	1.59	0.08	2.46	3.95	-	8.93	7
7	36. Ivigtut.	9	9.6 0.1	0.2 0.1	30.4 0.6	44.8 0.6	-	16.4 0.2	101.4	1.58	0.06	2.61	3.81	-	9.09	7
	Ourayite.															
8	ROM M4100. Colorado, USA.	11	12.5 0.6	0.5 0.1	29.5 1.5	41.4 1.0	0.2 0.1	16.0 0.3	100.1	3.04	0.21	3.73	5.19	-	13.07	11
	Treasurite.															
9	R9714. Colorado, USA.	5	12.7 0.3	-	19.6 0.5	50.5 0.2	-	16.4 0.2	99.2	1.82	-	1.46	3.73	-	7.89	6
	Treasurite decomposition mineral.															
10	R9714.	8	13.8 0.5		19.0 0.9	49.8 1.3	-	16.3 0.4	98.9	$N_{(Cryst.)}$ not known						?
	Schirmerite. Colorado, USA.															
11	2571, grain 1.	1	10.3	-	19.0	54.4	-	16.4	100.1							
12	2571, 2.	1	10.7	-	18.9	53.5	-	16.7	99.8							
13	2571, 3.	1	9.8	-	22.0	53.2	-	16.5	101.5							
14	2571, 4.	1	9.6	-	22.9	51.9	-	16.3	100.7							
15	2571, 5.	1	9.7	-	24.8	50.6	-	15.7	100.8							
16	2571, 6.	1	9.3	-	25.1	49.7	-	16.3	100.4							
17	2571, 7.	1	9.7	-	22.3	49.5	-	16.0	97.5							
18	2571, 8.	1	9.8	-	25.9	49.3	-	16.3	101.3							
19	2571, 9.	1	9.4	-	27.1	48.2	-	16.4	101.1							
20	2571, 10.	1	9.2	-	28.9	46.9	-	16.3	101.3							
21	2571, 11.	1	9.4	-	28.3	46.7	-	16.2	100.6	$N_{(Cryst.)}$ not defined						
22	2571, 12.	1	9.2	-	29.2	46.6	-	16.1	101.1							
23	2571, 13.	1	9.1	-	28.6	46.3	-	15.7	99.7	Unit cell content						
24	2571, 14.	1	9.2	-	29.4	45.3	-	16.2	100.1	cannot be calculated						
25	2571, 15.	1	9.1	-	28.2	44.2	-	16.1	97.6							
26	2571, 16.	1	9.3	-	31.4	43.2	-	15.9	99.8							
27	2571, 17.	1	8.5	-	30.5	43.1	-	16.5	98.6							
28	2571, 18.	1	8.6	-	31.4	42.9	-	16.3	99.2							
29	2571, 19.	1	9.2	-	31.5	42.9	-	15.8	99.4							
30	2571, 20.	1	9.9	-	33.9	39.0	-	15.7	98.5							
		6														
31	2571. 6 spots analyzed in one grain.	6	9.9 0.2	-	22.5 0.8	51.8 0.6	-	16.8 0.3	101.0	$N_{(Cryst.)}$ not known						
32	2571. 10 spots analyzed in one grain.	10	9.0 0.4	-	25.7 1.4	47.2 1.0	-	16.1 0.3	98.0	- " -						
33	2571. 10 spots analyzed in one grain	10	8.8 0.3	-	31.1 0.6	42.8 0.6	-	15.8 0.2	98.5	- " -						
	Schirmerite decomposition mineral.															
34	2571. Average analysis of 7 grains in one area.	7	10.4 0.5	-	33.8 1.0	39.8 1.3	-	15.5 0.3	99.5	$N_{(Cryst.)}$ not known						?
35	2571. Average analysis of 14 grains in one area.	14	10.0 0.3	-	35.2 0.9	37.8 0.9	-	15.8 0.3	98.8	- " -						?
	Lillianite-gustavite series members.															
36	1440. Gladiator mine, USA.	11	9.1 0.2	0.3 0.2	18.4 1.0	54.9 0.8	1.1 0.3	18.4 1.0	102.2	0.95	0.05	1.00	2.95	0.10	6.45	4
37	1124. Alaska mine, USA.	12	8.8 0.4	0.2 0.1	18.7 1.2	54.5 1.5	0.2 0.2	17.2 0.3	99.6	0.94	0.04	1.04	3.00	0.02	6.18	4
38	58a. Ivigtut.	6	6.1 0.3	0.2 0.1	26.7 0.6	49.7 1.0	-	17.0 0.3	99.7	0.67	0.04	1.52	2.81	-	6.26	4
39	1973-188. Ivigtut. Average of host and lamellae.	9	6.6 0.3	0.1	27.1 0.9	50.5 0.3	-	17.1 0.3	101.3	0.71	0.02	1.51	2.79	-	6.15	4
40	1973-188. Ivigtut. *Host gustavite.*	12	7.3	nd.	22.8	51.2	-	nd.		0.80	nd.	1.30	2.90	-	nd.	4
41	1973-188. Exsolved lamellae.	13	5.0	nd.	31.5	46.0	-	nd.		0.55	nd.	1.82	2.63	-	nd.	4
42	LS 70-84-1. Sardinia, Italy. Is Lassinus mine.	11	4.5 0.5	0.4 0.2	32.4 0.9	46.4 1.4	-	16.6 0.2	100.3	0.50	0.07	1.86	2.64	-	6.16	4
43	2953. *Agenosawa mine, Japan.*	8	4.4 0.2	-	34.1 0.8	44.6 0.5	-	16.0 0.4	99.1	0.49	-	1.96	2.55	-	5.96	4
44	2568. Kingsgate, NSW. Australia.	6	3.4 0.3	0.1	38.0 0.8	42.2 0.5	1.1 0.1	16.1 0.2	100.8	0.37	0.02	2.15	2.37	0.11	5.89	4
45	2954. Agenosawa mine, Japan.	6	2.5 0.1	0.1	40.9 0.8	40.1 0.5	-	16.5 0.2	100.0	0.28	0.02	2.39	2.33	-	6.24	4
46	2801. Yakuki mine, Japan.	8	1.8 0.1	-	43.7 0.5	39.2 0.4	-	15.8 0.1	100.5	0.20	-	2.54	2.26	-	5.93	4
47	"Bursaite". Uludag, Turkey.	7	1.0 0.1	-	44.9 1.2	36.8 0.9	-	15.8 0.4	98.5	0.12	-	2.69	2.19	-	6.13	4
	"Gustavites" in section 1139, Colorado, USA.															
48	1139, grain 1.	1	8.8	0.6	16.9	54.4	3.0	17.4	101.1	0.91	0.10	0.91	2.90	0.27	6.05	4
49	1139, 2.	1	8.6	0.6	17.2	53.8	2.9	17.6	100.7	0.89	0.11	0.93	2.90	0.27	6.18	4
50	1139, 3.	1	8.8	0.5	17.2	52.1	3.2	17.4	99.2	0.93	0.09	0.94	2.83	0.30	6.16	4
51	1139, 4.	1	8.3	0.7	17.4	51.3	4.5	17.0	99.2	0.87	0.12	0.95	2.77	0.42	5.98	4
52	1139, 5.	1	8.9	0.5	17.4	53.2	2.9	17.5	100.4	0.93	0.09	0.94	2.86	0.27	6.13	4
53	1139, 6.	1	8.6	0.6	17.6	54.3	2.7	17.4	101.2	0.89	0.11	0.95	2.91	0.25	6.07	4
54	1139, 7.	1	9.1	0.4	17.6	53.9	2.6	17.5	101.1	0.94	0.07	0.95	2.87	0.24	6.08	4
55	1139, 8.	1	8.9	0.6	17.7	53 1	2.5	17.7	100.1	0.93	0.11	0.97	2.87	0.23	6.24	4
56	1139, 9.	1	8.1	0.6	19.7	54.2	2.9	17.2	99.7	0.86	0.11	1.08	2.79	0.27	6.11	4
57	1139, 10.	1	7.9	0.6	20.5	51.4	3.3	17.0	100.7	0.82	0.11	1.11	2.76	0.30	5.95	4
58	1139, 11.	1	8.3	0.4	20.6	49.0	4.2	17.6	100.1	0.86	0.07	1.12	2.63	0.39	6.12	4
59	1139, 12.	1	8.2	0.4	22.3	51.5	2.5	17.2	102.1	0.84	0.07	1.19	2.73	0.23	5.95	4
60	1139, 13.	1	7.5	0.5	22.6	49.7	2.6	16.6	99.5	0.79	0.09	1.25	2.72	0.24	5.91	4
61	1139, 14.	1	7.4	0.4	23.1	46.2	3.5	17.0	97.6	0.80	0.07	1.30	2.57	0.33	6.17	4
62	1139, 15.	1	7.3	0.5	24.0	48.0	2.6	16.9	99.3	0.78	0.09	1.33	2.64	0.25	6.06	4
63	1139, 16.	1	7.3	0.5	24.8	48.8	2.4	17.0	100.8	0.77	0.09	1.36	2.65	0.22	6.02	4
64	1139, 17.	1	7.4	0.6	24.9	47.0	2.7	16.9	99.5	0.79	0.11	1.38	2.58	0.25	6.05	4
65	1139, 18.	1	7.6	0.4	25.1	47.2	2.5	17.0	99.8	0.80	0.07	1.38	2.58	0.23	6.05	4
66	1139, 19.	1	7.1	0.6	25.7	47.2	2.5	17.0	100.0	0.75	0.11	1.42	2.59	0.24	6.08	4
	Heyrovskyite.															
67	2801. Yakuki mine, Japan.	14	1.3	-	58.3	25.0	-	14.7	99.3	0.23	-	5.45	2.32	-	8.87	7
	Unnamed lillianite homologue.															
68	1139. Colorado, USA.	16	8.9 0.5	0.6 0.1	31.2 1.7	42.8 1.7	0.8 0.4	16.3 0.3	100.6	$N_{(Cryst.)}$ not known						?

N. (Cryst.)	VALUES BASED ON Me(-Cu)/S				VALUES BASED ON Ag/Pb/Bi RATIO			
	N	L%	x	Δx	N	L%	x	Δx
5.5	5.27	67.2	1.10	0.05	5.12	67.2	1.05	0.01
5.5	4.76	69.6	0.96	0.15	5.23	69.4	1.12	0.05
5.5	5.43	66.8	1.15	0.18	4.91	66.8	0.97	0.05
5.5	5.29	72.8	1.20	0.06	5.11	73.0	1.14	0.02
5.5	5.29	72.2	1.19	0.04	5.17	72.3	1.15	0.01
7	7.56	70.7	1.97	0.53	5.78	71.3	1.35	0.12
7	6.34	67.9	1.47	0.04	6.18	67.9	1.42	0.01
11	10.18	69.7	2.85	0.05	9.92	69.8	2.76	0.01
6	6.90	86.8	2.13	0.16	6.33	87.8	1.90	0.04
?	8.09	86.5	2.63	0.19	7.30	87.5	2.32	0.05
	6.00	89.1	1.78	0.58	4.43	95.4	1.16	0.13
	5.00	92.5	1.39	0.11	4.69	93.3	1.27	0.03
	6.17	83.6	1.74	0.60	4.52	88.2	1.11	0.14
	6.41	81.2	1.79	0.64	4.62	85.2	1.12	0.14
	10.93	75.8	3.38	2.02	4.94	80.5	1.18	0.31
	6.05	77.3	1.57	0.40	4.87	79.2	1.14	0.10
	5.73	82.1	1.53	0.28	4.91	84.0	1.23	0.07
	6.99	75.7	1.89	0.56	5.23	77.6	1.25	0.13
	6.14	73.9	1.53	0.28	5.25	74.7	1.23	0.07
	6.60	70.4	1.62	0.35	5.46	70.9	1.23	0.09
	6.71	71.2	1.68	0.35	5.56	71.8	1.28	0.09
	7.49	69.70	1.91	0.60	5.52	70.3	1.24	0.14
	8.72	69.9	2.35	1.00	5.47	70.8	1.23	0.20
	6.25	69.0	1.47	0.15	5.75	69.1	1.30	0.04
	5.16	70.2	1.11	0.19	5.80	69.9	1.33	0.06
	7.65	65.5	1.85	0.35	6.38	65.4	1.43	0.08
	4.25	65.0	0.73	0.45	5.78	65.4	1.24	0.16
	5.08	63.9	0.99	0.25	5.95	64.2	1.27	0.08
	7.83	65.1	1.90	0.39	6.38	65.0	1.42	0.09
	8.28	61.2	1.92	0.01	8.32	61.2	1.94	0.00
	4.92	85.1	1.24	0.06	4.74	85.7	1.18	0.02
	5.30	76.7	1.25	0.07	5.09	76.0	1.17	0.02
	6.76	64.9	1.55	0.19	6.08	64.8	1.32	0.05
?	12.48	62.9	3.30	0.82	8.57	62.4	2.05	0.16
?	8.00	59.2	1.78	0.21	9.06	59.6	2.10	0.06
4	2.45	109.0	0.38	0.55	3.75	103.0	0.90	0.21
4	3.25	109.3	0.68	0.23	3.80	100.1	0.90	0.07
4	2.96	78.6	0.38	0.31	3.67	74.7	0.62	0.10
4	3.35	76.9	0.52	0.19	3.81	75.1	0.68	0.06
4					3.77	86.4	0.76	0.12
4					3.82	58.7	0.53	0.16
4	3.31	53.9	0.35	0.15	3.66	55.8	0.46	0.05
4	4.22	52.6	0.59	0.15	3.85	51.0	0.47	0.04
4	4.59	45.7	0.59	0.35	3.75	40.2	0.35	0.09
4	3.04	10.2	0.06	0.35	3.89	29.1	0.28	0.12
4	4.35	26.9	0.32	0.20	3.86	21.0	0.20	0.05
4	3.43	3.1	0.02	0.16	3.82	12.2	0.11	0.05
4	3.74	107.9	0.94	0.15	3.41	116.1	0.82	0.04
4	3.23	116.9	0.72	0.06	3.41	112.5	0.79	0.02
4	3.30	114.6	0.74	0.11	3.54	109.4	0.84	0.03
4	4.11	101.5	1.07	0.37	3.32	113.9	0.75	0.10
4	3.41	111.9	0.79	0.06	3.54	109.2	0.84	0.02
4	3.66	106.9	0.88	0.11	3.42	111.3	0.79	0.03
4	3.62	107.8	0.87	0.01	3.60	108.0	0.87	0.00
4	3.04	121.0	0.63	0.24	3.61	106.9	0.86	0.08
4	3.51	101.6	0.77	0.01	3.53	101.2	0.78	0.00
4	4.24	92.6	1.04	0.35	3.46	100.7	0.73	0.09
4	3.30	103.1	0.67	0.15	3.64	97.8	0.80	0.05
4	4.25	88.7	1.00	0.23	3.72	92.6	0.80	0.06
4	4.48	85.3	1.06	0.37	3.62	90.7	0.73	0.10
4	3.29	91.3	0.59	0.19	3.74	86.8	0.76	0.06
4	3.70	85.1	0.72	0.02	3.74	84.9	0.74	0.01
4	3.92	82.5	0.79	0.07	3.75	83.4	0.73	0.02
4	3.78	82.1	0.73	0.04	3.88	81.6	0.77	0.01
4	3.75	82.1	0.72	0.09	3.98	80.9	0.80	0.03
4	3.65	80.5	0.66	0.08	3.83	79.6	0.73	0.02
7	8.10	14.8	0.45	0.37	6.68	9.6	0.22	0.09
?	5.96	65.7	1.30	0.20	5.90	65.7	1.28	0.01

Table 3. X-ray powder data on vikingite in polished section 41 (Gandolfi camera. Cu Kα-rad.)

I	^{d}hkl Meas.	^{d}hkl Calc.	Indices
4	3.62	3.73	121
10	3.40	3.42	260
		3.38	141
2	3.30	3.31	270
4	3.05	3.05	270
1	3.00	2.99	311
5	2.91	2.96	280
2	2.80	2.75	280
1	2.50	2.54	361
		2.53	351
		2.52	460
1	2.30	2.31	191
1	2.25	2.25	191
1	2.14	2.15	1.10.1
4	2.10	2.09	1.10.1
8	2.06	2.07	660
3	1.991		
3	1.924		
4	1.877		
1	1.840		
2	1.802		
9	1.754		
2	1.703		
2	1.686		
1	1.478		
1	1.454		
2	1.425		
1	1.407		
1	1.384		
1	1.355		
2	1.331		
2	1.309		
3	1.298		
1	1.202		
3	1.181		

Powder data obtained from one fragment isolated from polished section 41 are listed in table 3. Weissenberg photographs of the same fragment gave a = 13.603(6)Å, b = 25.248(7)Å, c = 4.112(4)Å and γ = 95.55(3)° (M-KM77b). A weak 8Å level (2×c) was recognized in the x-ray films. Extinction and intensity relationships permit B2/m and Bm for the very pronounced 4Å subcell and P2/a or Pa for the 8Å unit cell. The crystallographic data indicate $N_1 = 4.0$, $N_2 = 7.0$ and $N_{average} = 5.5$. The proposed structure for the mineral (M-KM77b) is shown in fig. 2.

Weissenberg photographs of fragments of a vikingite grain isolated from polished sections 58a and 31 showed twinning of the mineral on (010). Twin lamellae parallel to [001] were often observed.

Microprobe analyses of vikingite are listed in table 1, 1–5 and plotted in fig. 3, 1–5.

TABLE 2. PUBLISHED CHEMICAL COMPOSITIONS OF Ag-Pb-Bi-(Cu-Sb-Se-Te)-S MINERALS.

Analysis No.	DESCRIPTION	Wt. % - VALUES									UNIT CELL FORMULA (Z=4) BASED ON SUM OF METALS (-Cu) = $N_{Cryst.}$ + 1								N. (Cryst.)
		Ag	Cu	Pb	Bi	Sb	S	Se	Te	Sum	Ag	Cu	Pb	Bi	Sb	S	Se	Te	
	Nedachi et al., (1973)																		
	Members of the lillianite-gustavite series																		
69	Anal. 7, table 2 in their paper	2.2	-	43.8	38.5	-	16.5	-	-	101.0	0.24	-	2.54	2.21	-	6.18	-	-	4
70	8,	4.2	-	37.7	42.1	-	15.8	-	-	99.8	0.46	-	2.15	2.38	-	5.83	-	-	4
71	9,	3.9	0.1	37.2	43.4	-	16.4	-	-	101.0	0.42	0.02	2.12	2.45	-	6.04	-	-	4
72	10,	3.7	0.1	36.0	44.8	-	16.4	-	-	101.2	0.41	0.02	2.06	2.54	-	6.13	-	-	4
73	11,	9.4	-	24.3	48.3	-	16.5	-	-	98.5	1.00	-	1.35	2.65	-	5.91	-	-	4
74	12,	8.4	0.1	23.0	51.0	-	16.5	-	-	99.0	0.90	0.02	1.28	2.82	-	5.94	-	-	4
75	13,	9.1	0.1	23.5	52.1	-	16.7	-	-	101.5	0.94	0.02	1.27	2.79	-	5.82	-	-	4
76	14,	9.1	0.1	23.6	52.3	-	16.8	-	-	101.9	0.94	0.02	1.27	2.79	-	5.84	-	-	4
77	15,	8.9	0.1	22.7	53.4	-	17.2	-	-	102.3	0.92	0.02	1.22	2.85	-	5.99	-	-	4
78	16,	9.1	0.1	21.1	55.8	-	16.9	-	-	103.0	0.93	0.02	1.12	2.95	-	5.81	-	-	4
79	17,	9.5	0.2	18.9	55.4	-	16.3	-	-	100.3	0.99	0.04	1.03	2.98	-	5.72	-	-	4
80	18,	9.3	0.1	19.8	52.8	-	16.7	-	-	98.7	0.99	0.02	1.10	2.91	-	5.99	-	-	4
	Czomanske and Hall (1975)																		
	Type III (Gustavite ?)																		
81	Anal. A561.D, table 2 in their paper	9.2	-	19.7	47.0	4.7	16.2	2.2	0.13	99.1	0.96	-	1.07	2.53	0.43	5.69	0.31	0.01	4
82	H-2.B,	9.0	-	19.7	47.5	4.4	16.4	2.0	0.07	99.1	0.94	-	1.08	2.57	0.41	5.79	0.29	0.01	4
83	H-2.D,	8.9	-	20.1	48.6	4.0	16.2	2.0	0.10	99.9	0.93	-	1.09	2.61	0.37	5.68	0.28	0.01	4
	Type I (Cosalite ?)																		
84	Anal. A561.C, table 2 in their paper	2.4	-	40.4	30.2	7.5	16.3	1.4	0.19	98.4	0.26	-	2.30	1.71	0.73	6.00	0.21	0.02	4
85	A561.A,	2.9	-	39.1	31.0	7.7	16.3	1.7	0.13	98.8	0.31	-	2.21	1.74	0.74	5.95	0.25	0.01	4
86	A561.D,	3.0	-	37.9	31.0	7.3	16.1	1.7	0.19	97.2	0.33	-	2.18	1.77	0.72	5.99	0.26	0.02	4
	Type II																		
87	Anal. H-2.A, table 2 in their paper	9.6	-	25.5	41.7	3.6	15.4	2.9	0.21	98.9	1.31	-	1.81	2.94	0.44	7.08	0.54	0.02	5.5 ?
88	H-2.C,	9.5	-	25.8	42.1	3.3	15.5	2.3	0.21	98.7	1.30	-	1.83	2.97	0.40	7.12	0.43	0.02	5.5 ?
	Type unnamed																		
89	Anal. A561.E, table 2 in their paper	9.4	-	22.2	43.0	4.4	16.1	2.5	0.10	97.7	1.30	-	1.60	3.07	0.54	7.48	0.47	0.01	5.5 ?
	Type IV																		
90	Anal. DM1.D, table 2 in their paper	7.3	-	39.3	31.6	0.11	10.6	9.0	0.79	98.7	1.32	-	3.71	2.95	0.02	6.46	2.23	0.12	7
91	DM1A.B,	6.8	-	38.9	33.9	0.09	10.9	9.1	0.64	100.3	1.22	-	3.63	3.14	0.01	6.57	2.23	0.10	7
92	D130A.D,	6.4	-	37.3	34.6	0.13	10.9	8.8	0.59	98.7	1.17	-	3.55	3.26	0.02	6.70	2.20	0.09	7
93	D130A.1,	6.4	-	37.3	34.8	0.13	11.4	8.1	0.59	98.7	1.17	-	3.54	3.27	0.02	6.99	2.02	0.09	7
94	3501.4,	8.4	-	33.2	36.5	-	11.9	7.4	0.75	99.3	1.51	-	3.11	3.39	-	7.19	1.82	0.11	7
95	DM1.P,	11.0	-	29.4	36.9	0.08	10.9	10.0	1.00	99.3	1.94	-	2.70	3.35	0.01	6.46	2.41	0.15	7
96	DM1.X2,	10.7	-	29.2	37.5	0.14	10.2	10.3	0.95	99.0	1.89	-	2.68	3.41	0.02	6.05	2.48	0.14	7
97	DM1.X1,	10.3	-	29.4	37.8	0.10	10.6	10.0	0.87	99.1	1.82	-	2.71	3.45	-	6.31	2.42	0.13	7
98	3501.2,	8.1	-	32.2	37.9	-	11.8	7.8	0.64	98.4	1.46	-	3.02	3.52	-	7.15	1.92	0.10	7
99	3501.3,	8.9	-	32.4	38.3	-	11.5	8.0	0.71	99.8	1.56	-	2.96	3.47	-	6.80	1.92	0.11	7
100	3501.1,	9.1	-	29.0	40.1	-	12.4	7.2	0.64	98.4	1.62	-	2.69	3.69	-	7.43	1.75	0.10	7
	Type II, annealed																		
101	Anal. H-2. at 250°C, table 4 in their paper	9.5	-	26.7	42.9	2.9	15.7	2.2	0.21	100.1	1.28	-	1.88	2.99	0.34	7.14	0.41	0.02	5.5 ?
102	H-2. at 310°C,	5.5	-	41.7	31.9	2.9	15.4	2.4	0.20	99.9	0.77	-	3.05	2.31	0.36	7.28	0.46	0.02	5.5 ?
103	H-2. at 310°C,	5.2	-	44.1	30.0	3.1	14.8	2.3	0.25	99.8	0.73	-	3.22	2.17	0.38	6.98	0.44	0.03	5.5 ?
	Type I (Cosalite ?), annealed																		
104	Anal. A561 at 310°C, table 4 in their paper	2.4	-	43.4	28.5	7.0	16.0	1.4	0.12	98.8	0.26	-	2.46	1.61	0.68	5.88	0.21	0.01	4
	Type IV. Shreds, annealed																		
105	Anal. DM1, 250°C, table 4 in their paper	2.1	-	14.8	47.2	0.2	4.3	6.8	23.2	98.4	0.49	-	1.79	5.67	0.04	3.37	2.16	4.57	7 ?
106	DM1, 250°C,	1.9	-	19.4	45.9	0.2	4.6	7.6	20.5	100.1	0.43	-	2.25	5.28	0.04	3.45	2.32	3.87	7 ?
107	DM1, 310°C,	3.2	-	11.4	48.0	0.18	4.5	6.7	24.3	98.3	0.75	-	1.39	5.82	0.04	3.55	2.15	4.82	7 ?
108	DM1, 310°C,	3.1	-	19.6	45.4	0.15	4.6	7.7	20.5	101.1	0.67	-	2.21	5.08	0.03	3.36	2.28	3.76	7 ?
	Type IV. Hosts, annealed																		
109	Anal. DM1, 250°C, table 4 in their paper	7.4	-	41.0	30.6	0.2	10.3	9.0	0.68	99.2	1.32	-	3.82	2.83	0.03	6.20	2.20	0.10	7 ?
110	DM1, 310°C,	6.8	-	40.5	30.9	0.2	11.0	8.2	0.68	98.3	1.24	-	3.83	2.90	0.03	6.73	2.04	0.10	7 ?
111	DM1, 310°C,	6.2	-	42.5	31.4	0.2	10.3	9.1	0.90	100.6	1.11	-	3.96	2.90	0.03	6.20	2.22	0.14	7 ?
	Ontoev (1959). Lillianite.																		
112	Anal. 1, table 2 in his paper	2.2	-	48.3	33.2	0.2	15.5	-	-	99.4	0.25	-	2.82	1.92	0.01	5.84	-	-	4
	Analyses by Dr. Kieft - unpublished																		
113	Anal. 1	5.5	0.25	33.5	45.2	-	15.55	-	-	100.0	0.60	0.05	1.88	2.52	-	5.65	-	-	4
114	Anal. 2	5.4	0.35	30.55	47.05	-	16.7	-	-	100.1	0.59	0.07	1.74	2.66	-	6.16	-	-	4
	Nuffield (1975). Gustavite																		
115	Anal. 3, table 5 in his paper	7.67	0.18	22.44	55.03	-	15.32	-	-	100.64	0.80	0.03	1.22	2.97	-	5.40	-	-	4
116	4,	7.15	0.20	22.39	55.23	-	16.30	-	-	101.27	0.76	0.04	1.23	3.01	-	5.79	-	-	4
	Harris and Chen (1975). Gustavite.																		
117	Anal. 1, table 4 in their paper	8.9	-	18.9	52.0	3.3	17.7	-	-	100.8	0.92	-	1.01	2.77	0.30	6.14	-	-	4
118	2,	7.8	-	20.2	50.3	3.6	17.6	-	-	99.5	0.82	-	1.11	2.73	0.34	6.24	-	-	4
119	3,	9.4	-	19.9	53.2	-	17.4	-	-	99.9	1.00	-	1.10	2.91	-	6.20	-	-	4
	Karup-Møller (1972). Gustavite.																		
120	Anal. 1-1821, table 5 in his paper	9.2	0.4	18.3	53.1	3.1	17.5	-	-	101.6	0.94	0.07	0.97	2.80	0.28	6.02	-	-	4
121	2-1821,	9.2	0.4	18.2	53.1	2.5	17.6	-	-	100.0	0.95	0.07	0.98	2.84	0.23	6.13	-	-	4
	Klominsky et al., (1971).																		
	"Bursaite"																		
122	Anal. 15, table 3 in their paper	1.0	-	45.0	38.5	-	14.7	-	-	100.4	0.11	-	2.64	2.24	-	5.58	-	-	4
123	16,	1.0	-	44.6	39.3	-	14.7	-	-	101.0	0.11	-	2.61	2.28	-	5.56	-	-	4
	Heyrovskyite																		
124	Anal. 4, table 3 in their paper	1.1	-	58.6	24.9	-	14.5	-	-	97.5	0.20	-	5.49	2.31	-	8.78	-	-	7
125	6,	1.1	-	57.4	25.9	-	14.5	-	-	98.9	0.20	-	5.39	2.41	-	8.80	-	-	7
126	5,	1.1	-	58.0	26.3	-	14.5	-	-	100.7	0.20	-	5.38	2.42	-	8.70	-	-	7
127	3,	2.5	-	54.7	27.7	-	14.4	-	-	100.1	0.44	-	5.03	2.53	-	8.56	-	-	7
128	2,	2.5	-	53.6	28.3	-	14.4	-	-	99.7	0.44	-	4.96	2.60	-	8.61	-	-	7
	Syritso and Senderova (1964). Lillianite ?																		
129	Anal. 1, table 1 in their paper	2.17	0.14	49.61	31.31	0.57	15.35	-	-	99.15	0.24	0.03	2.89	1.81	0.06	5.78	-	-	4
130	2,	2.39	0.57	49.75	30.44	1.01	15.55	-	-	99.71	0.27	0.11	2.88	1.75	0.10	5.82	-	-	4
	Borodaev and Mozgowa (1971). Gustavite.																		
131	Anal. 16, table 1 in their paper.	8.9	0.5	18.2	56.2	-	16.2	-	-	100.0	0.92	0.09	0.98	3.01	-	5.65	-	-	4

N. (Cryst.)	VALUES BASED ON Me(-Cu)/S				VALUES BASED ON Ag/Pb/Bi RATIO			
	N	L%	x	Δx	N	L%	x	Δx
4	3.22	6.2	0.04	0.34	4.08	24.0	0.25	0.12
4	5.00	47.2	0.71	0.31	4.20	43.6	0.48	0.08
4	3.81	42.5	0.38	0.05	3.94	43.5	0.42	0.02
4	3.43	42.6	0.31	0.11	3.69	45.0	0.38	0.03
4	4.51	80.7	1.01	0.18	5.05	79.4	1.21	0.06
4	4.30	84.4	0.97	0.04	4.21	84.8	0.94	0.01
4	5.07	82.4	1.26	0.24	4.42	84.5	1.02	0.06
4	4.95	82.7	1.22	0.20	4.41	84.5	1.02	0.05
4	4.04	88.5	0.90	0.05	4.17	87.7	0.95	0.02
4	5.14	87.9	1.38	0.47	3.96	94.1	0.92	0.12
4	5.95	89.2	1.76	0.77	4.02	98.5	1.00	0.17
4	4.03	94.8	0.96	0.07	4.22	93.3	1.04	0.02
4	3.96	96.8	0.95	0.01	3.98	96.6	0.96	0.00
4	3.68	99.6	0.84	0.09	3.91	97.0	0.93	0.03
4	4.22	93.8	1.04	0.15	3.87	96.7	0.90	0.04
4	2.96	14.3	0.07	0.28	3.60	30.2	0.24	0.09
4	3.15	27.5	0.16	0.21	3.63	35.8	0.29	0.07
4	2.99	25.2	0.13	0.28	3.64	37.5	0.31	0.09
5.5 ?	4.54	78.5	1.00	0.24	5.30	77.1	1.27	0.08
5.5 ?	5.01	76.9	1.16	0.09	5.28	76.4	1.25	0.03
5.5 ?	3.35	94.9	0.64	0.46	4.64	85.4	1.13	0.16
7	8.58	47.8	1.57	0.02	8.70	47.9	1.60	0.01
7	7.65	48.2	1.35	0.09	7.28	47.8	1.26	0.02
7	7.23	49.3	1.29	0.18	6.57	48.4	1.11	0.05
7	6.45	48.4	1.08	0.02	6.52	48.5	1.10	0.01
7	6.10	57.2	1.17	0.34	7.53	58.2	1.61	0.11
7	6.96	66.1	1.64	0.58	10.2	66.2	2.71	0.21
7	11.2	66.4	3.04	0.35	9.34	66.4	2.44	0.08
7	8.19	65.9	2.04	0.10	8.72	65.9	2.22	0.03
7	5.97	58.9	1.17	0.20	6.75	59.5	1.41	0.06
7	8.93	61.4	2.13	0.37	7.38	60.9	1.64	0.09
7	5.20	66.1	1.06	0.40	6.74	66.2	1.60	0.13
5.5 ?	5.23	75.2	1.21	0.03	5.33	75.1	1.25	0.01
5.5 ?	4.18	34.3	0.38	0.48	5.83	42.4	0.81	0.17
5.5 ?	5.86	38.0	0.73	0.07	6.12	38.7	0.80	0.02
4	3.62	21.4	0.17	0.14	3.96	26.5	0.26	0.04
7 ?	2.70	123.5	0.43	0.41	2.07	543.0	0.19	0.11
7 ?	3.84	79.8	0.74	0.96	2.28	126.5	0.17	0.16
7 ?	2.19	329.9	0.32	0.04	2.13	436.2	0.29	0.01
7 ?	4.65	78.7	1.04	1.14	2.60	100.5	0.30	0.24
7 ?	15.5	49.1	3.30	1.16	9.43	46.5	1.73	0.21
7 ?	8.23	45.1	1.41	0.04	8.44	45.3	1.46	0.01
7 ?	13.6	46.3	2.69	1.33	7.78	42.1	1.22	0.23
4	4.93	20.1	0.30	0.00	4.92	20.0	0.29	0.00
4	6.73	59.6	1.41	0.97	4.21	56.5	0.62	0.20
4	3.31	61.5	0.40	0.22	3.83	62.6	0.57	0.07
4	11.64	78.3	3.77	3.49	3.61	92.1	0.74	0.42
4	5.29	83.3	1.37	0.84	3.43	93.6	0.67	0.19
4	3.39	107.8	0.75	0.11	3.65	103.4	0.85	0.03
4	3.04	110.0	0.57	0.18	3.45	101.0	0.73	0.06
4	3.17	107.2	0.63	0.40	4.23	93.4	1.05	0.14
4	3.89	102.4	0.97	0.10	3.67	105.4	0.89	0.03
4	3.43	109.2	0.78	0.12	3.73	104.2	0.90	0.04
4	7.60	36.6	1.03	1.66	3.69	12.5	0.11	0.29
4	8.00	38.4	1.15	1.90	3.62	12.8	0.10	0.31
7	9.30	16.9	0.62	0.73	6.57	8.2	0.19	0.15
7	9.02	18.1	0.63	0.77	6.23	8.5	0.18	0.16
7	10.48	20.7	0.88	1.19	6.19	8.4	0.18	0.22
7	13.30	29.3	1.65	1.73	6.68	18.1	0.42	0.27
7	12.13	29.5	1.49	1.53	6.44	18.6	0.41	0.26
4	5.40	20.6	0.35	0.08	5.16	18.9	0.30	0.02
4	5.06	18.4	0.28	0.08	5.32	20.3	0.34	0.02
4	5.66	90.9	1.66	0.83	3.71	103.4	0.89	0.18

In *polished sections 2 and 41* vikingite is associated with cosalite and small amounts of galena. Microprobe analyses of the cosalite in polished section 2 are listed in table 8, C1 and plotted in fig. 3, C1. The vikingite fragment investigated by the Weissenberg and the Gandolfi methods was removed from a grain in polished section 41. The remnants of this grain in the polished sections were analyzed in 8 different spots, table 1, 2. The analysis is very close to that determined on 8 different grains in the same polished section (table 1, 1). The last is plotted in fig. 3, 1.

In *polished section 31* vikingite occurs associated with cosalite (fig. 3, C2) or as lamellae in galena. Vikingite was identified by single crystal studies. Microprobe analyses on vikingite associated with cosalite and galena gave the results listed in table 1, 4 and 5. The difference in the average composition of vikingite in the two associations lies within the experimental error.

The greatest difference in chemical composition was found between analyses 3 and 4, and is due to a small degree of the $Ag^{+} + Bi^{+++} \leftrightarrow 2Pb^{++}$ substitution. The analyses suggest:

Polished section 2
$Ag_{0.97}Cu_{0.05}Pb_{1.97}Bi_{2.97}S_{6.91}$, N (chemical) = 4.91,
L % = 66.8, x = 0.97 and Δx = 0.05.
Polished section 31
$Ag_{1.14}Cu_{0.05}Pb_{1.83}Bi_{3.14}S_{7.11}$, N (chemical) = 5.11,
L % = 73.0, x = 1.14 and Δx = 0.02.
The ideal formula is
$Ag_{1.00}Pb_{2.50}Bi_{3.00}S_{7.5}$, Z = 4, N (cryst.) = 5.5,
L % = 57.1 and x = 1.00.

Eskimoite

Eskimoite, like vikingite, is only known from the Ivigtut gustavite-cosalite-galena paragenesis. It was named after the first inhabitants of Greenland, the Eskimos.

Eskimoite is lamellar and has an average grain size of 0.5 mm. It is optically indistinguishable from gustavite and vikingite. Reflectance values recorded in air at the four principal wave lengths are according to Vendrell-Saz et al. (in press.): 481 (λnm) = 45.4–48.2, 546 (λnm) = 43.7–46.5, 589 (λnm) = 42.8–45.6 and 644 (λnm) = 42.0–44.8.

The micorindentation hardness measured on 20 grains (VHN_{50gr}) ranges from 162 to 223 and averages 191±20.

Gandolfi powder data for eskimoite are listed

TABLE 2, CONTINUED.

Analysis No.	DESCRIPTION	Wt. % - VALUES Ag	Cu	Pb	Bi	Sb	S	Se	Te	Sum	UNIT CELL FORMULA (Z=4) BASED ON SUM OF METALS (-Cu) = $N_{Cryst.}$ + 1 Ag	Cu	Pb	Bi	Sb	S	Se	Te	N (Cryst.)
	Ontoev et al., (1972).																		
	"Se-free and Ag-bearing wittite"																		
132	Anal. 1, table 3 in their paper	5.1	-	29.3	49.0	-	15.1	-	-	98.5	0.56	-	1.67	2.77	-	5.56	-	-	4
133	2,	5.1	-	30.2	49.1	-	16.0	-	-	100.4	0.55	-	1.70	2.74	-	5.82	-	-	4
134	3,	5.1	-	30.7	49.2	-	15.8	-	-	100.8	0.55	-	1.72	2.73	-	5.72	-	-	4
	Mozgova et al., (1976).																		
	Heyrovskyite																		
135	Anal. 1, table 1 in their paper	1.9	0.1	56.1	28.3	0.5	15.6	-	-	102.5	0.33	0.03	5.06	2.53	0.08	9.10	-	-	7
136	2,	1.05	-	54.26	28.81	0.11	15.24	0.24	-	99.71	0.19	-	5.11	2.69	0.02	9.27	0.06	-	7
137	3,	1.01	1.05	54.53	28.18	-	15.31	-	-	100.08	0.18	0.32	5.17	2.65	-	9.38	-	-	7
138	3a,	1.8	-	54.4	27.2	-	14.0	-	-	97.4	0.33	-	5.13	2.54	-	8.53	-	-	7
	Large and Mumme (1975).																		
	Se-heyrovskyite																		
139	Anal. 1, table 6 in their paper	-	0.2	56.6	27.0	-	10.3	7.1	-	101.2	-	0.06	5.43	2.57	-	6.36	1.78	-	7
140	2,	-	-	54.0	28.1	-	11.1	6.8	-	100.0	-	-	5.28	2.72	-	7.01	1.74	-	7
141	3,	-	-	55.2	27.0	-	11.2	6.8	-	100.0	-	-	5.39	2.61	-	7.06	1.77	-	7
142	4,	-	-	54.6	26.6	-	11.8	6.7	-	99.7	-	-	5.39	2.61	-	7.53	1.74	-	7

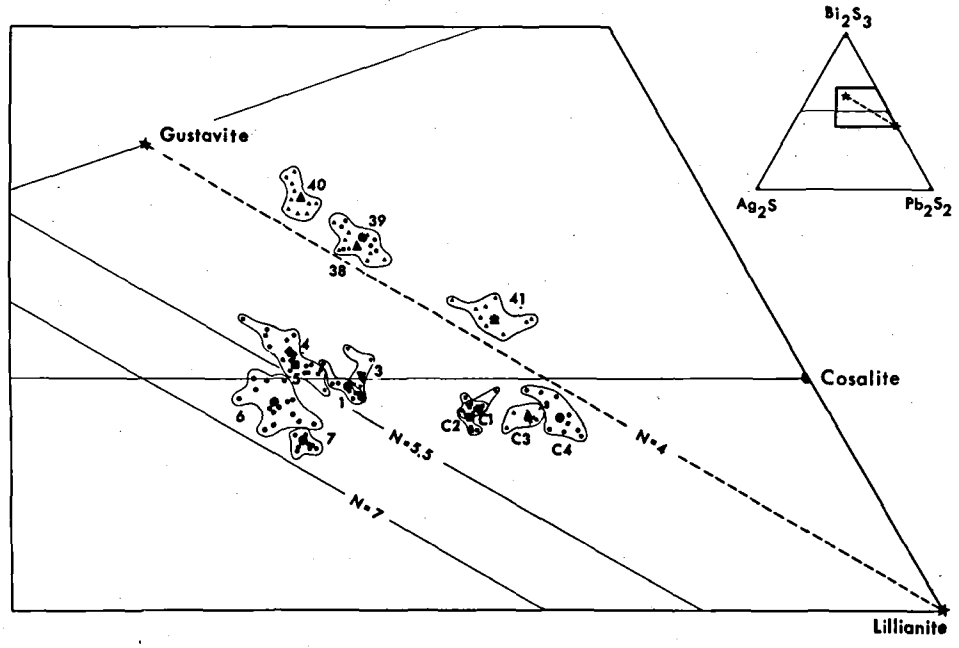

Fig. 3. Microprobe analysis plots representing members of the Ivigtut gustavite-cosalite-galena paragenesis. Small symbols within an outlined area represent analyses on individual mineral grains representing one distinct mineral species in one polished section. Large symbols represents the average of these values. Numbers refer to analysis numbers in the left column in table 1 and table 8.

No. 1, 3, 4 and 5: vikingite in polished section 41, 2 and 31. 4: vikingite lamellae in galena matrix in polished section 31. 5: vikingite in areas surrounding the galena matrix-vikingite in polished section 31. 6 and 7: eskimoite in polished section 35 and 36. 38 and 39: average composition of gustavite host and exsolved phase in polished sections 58a and 1973–188. 40: gustavite host in polished section 1973–188 and 41: exsolved phase in this (40 and 41 are reproduced from KM70). C1 and C2: cosalite associated with vikingite in polished sections 2 and 31. C3 and C4: cosalite associated with gustavite in polished sections 1973–188 and 58a.

N. (Cryst.)	VALUES BASED ON Me(-Cu)/S				VALUES BASED ON Ag/Pb/Bi RATIO			
	N	L%	x	Δx	N	L%	x	Δx
4	7.86	66.5	1.95	1.92	3.52	66.4	0.51	0.32
4	5.03	65.2	0.99	0.64	3.56	64.6	0.50	0.15
4	5.97	64.8	1.29	1.04	3.58	63.6	0.50	0.22
7	6.30	15.8	0.34	0.08	6.02	14.4	0.29	0.02
7	5.03	6.04	0.09	0.10	5.36	8.98	0.15	0.00
7	4.81	2.06	0.03	0.21	5.49	8.54	0.48	0.06
7	14.04	28.2	1.70	2.17	6.22	14.0	0.29	0.31
7	42.3	29.5	5.96	11.91	5.23	•	•	•
7	9.29	20.6	0.75	1.50	4.88	•	•	•
7	8.65	17.3	0.58	1.15	5.12	•	•	•
7	5.71	4.97	0.09	0.18	5.14	•	•	•

• Computations meaningless

in table 4. Cell dimensions obtained from Weissenberg photographs gave: a = 13.459(5)Å, b = 30.194(8)Å, c = 4.100(5)Å and $\gamma = 93.35(5)°$. Extinction and intensity relationships permit the space group possibilities B2/m and Bm. Crystallographic $N_1 = 5$, $N_2 = 9$ and $N_{average} = 7.0$. (Note that eskimoite has the same average crystallographic N as heyrovskyite. Therefore hypothetical varieties of the two minerals with similar L % and x cannot be distinguished from each other by means of only microprobe analyses). The Weissenberg photographs show twinning on (010). Twin lamellae parallel to the lamellar c-axis direction are often present.

Microprobe analyses for eskimoite are given in table 1, 6 and 1, 7, fig. 3, 6 and 3, 7. The analyses suggest:

Polished section 35

$Ag_{1.35}Cu_{0.08}Pb_{2.08}Bi_{3.35}S_{7.78}$, N (chemical) = 5.78, L % = 71.3, x = 1.35 and Δx = 0.12.

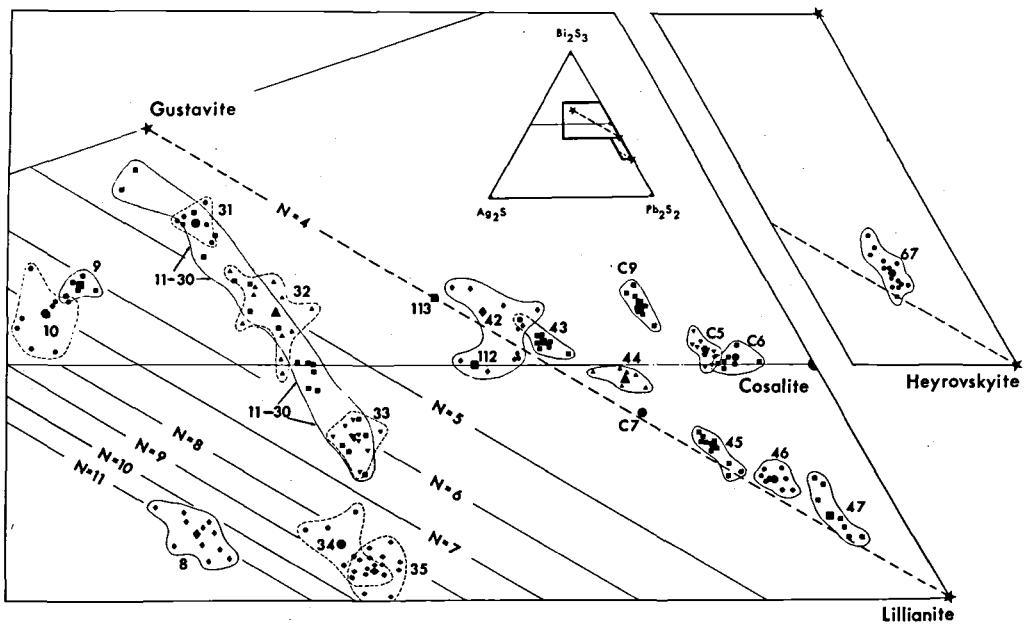

Fig. 4. General: see beginning of text to fig. 3. 8: ourayite. (Spl. ROM M4100). 9 and 10: treasurite and treasurite decomposition mineral (Spl. R9714). 11–30: schirmerite (polished section 2571). 31–33: analyses on different spots of three individual schirmerite grains. 34 and 35: schirmerite decomposition mineral in two different areas in the polished section 2571. 42: $^{3.66}Gus_{55.8}$ (polished section LS-70-B4-1). 112 and 113: two analyses (table 2, 113–114) by Kieft (unpublished) on the mineral in PS LS-70-134-1 represented by analysis no. 42. C7: composite of one cosalite grain in polished section LS-70-B4-1. 43 and 45: $^{3.85}Gus_{51.0}$ and $^{3.89}Gus_{29.1}$ from the Agenosawa mine, Japan. 44: $^{3.75}Gus_{40.2}$ (Kingsgate, Australia). C5 and C6: cosalite associated with $^{3.75}Gus_{40.2}$ and galenobismutite respectively (Kingsgate, Australia). 46: $^{3.86}Gus_{21.0}$ and 67: heyrovskyite ($^{6.68}Hey_{9.6}$) from Yakuki mine, Japan. 47: "bursaite" = $^{3.82}Gus_{12.2}$ (Bursa, Turkey).

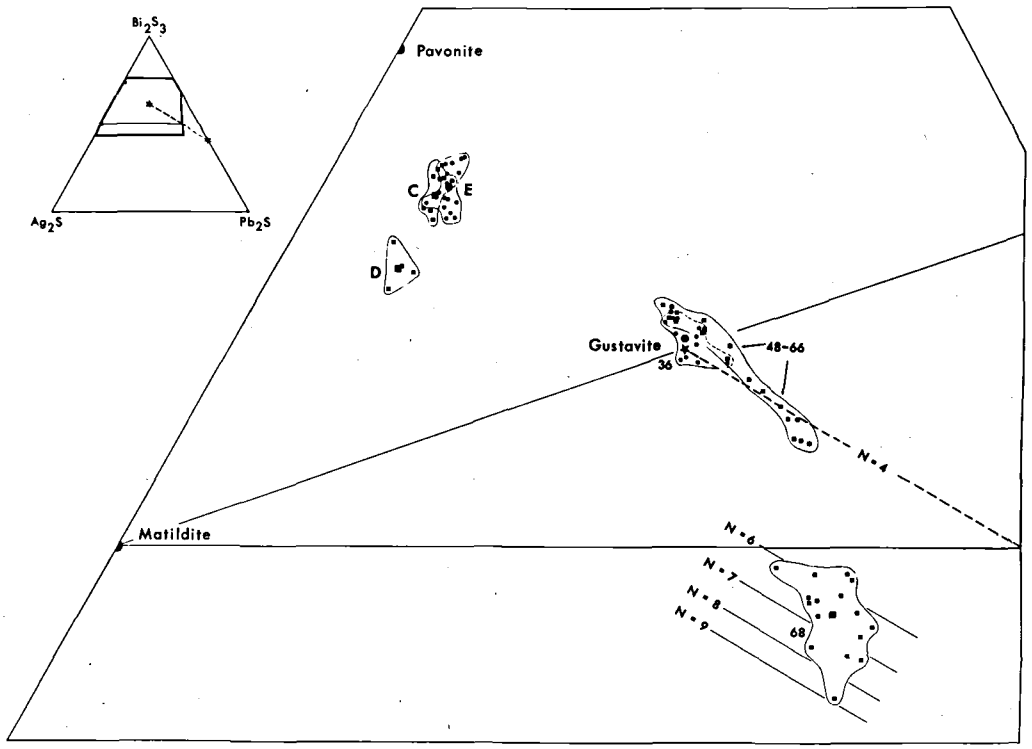

Fig. 5. General: see beginning of text to fig. 3. 48–66: 'gustavites' (Spl. 1139). 68: $^{5.90}L_{65.7}$ (Spl. 1139). C: pavonite (Spl. 1139). D: benjaminite (Spl. 1139). 36: $^{3.75}Gus_{103.0}$ (Spl. 1140). E: pavonite (Spl. 1140).

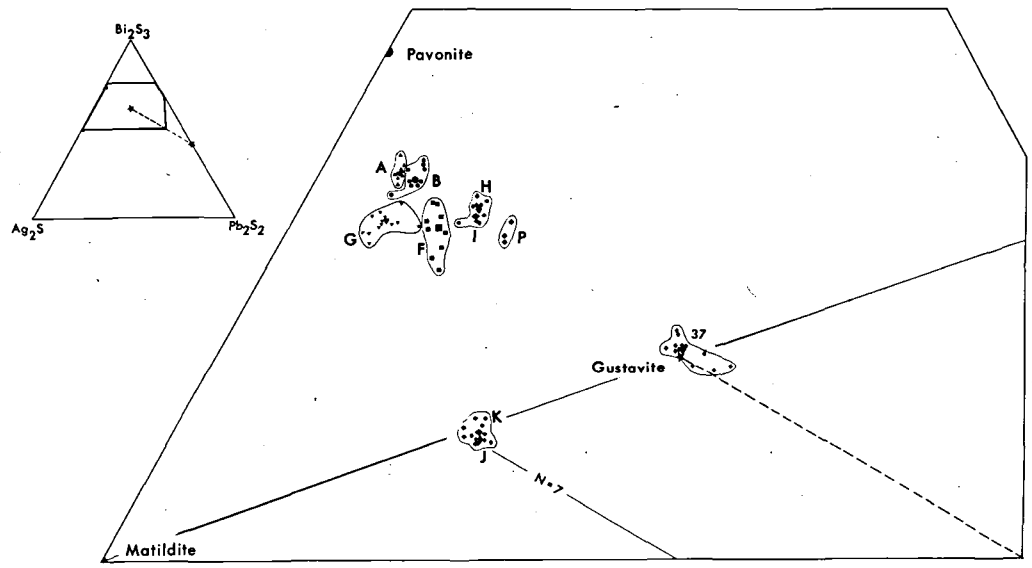

Fig. 6. General: see beginning of text to fig. 3. 37: $^{3.80}Gus_{100.1}$ (Spl. 1124). H and I: two host pavonite grains for K and J: exsolved lamellae (Spl. 1124). F: pavonite (?). (Spl. ROM M21003). G: benjaminite with submicroscopic gustavite (Spl. ROM M13805). P: analyses on pavonite by Nedachi et al. (1973).

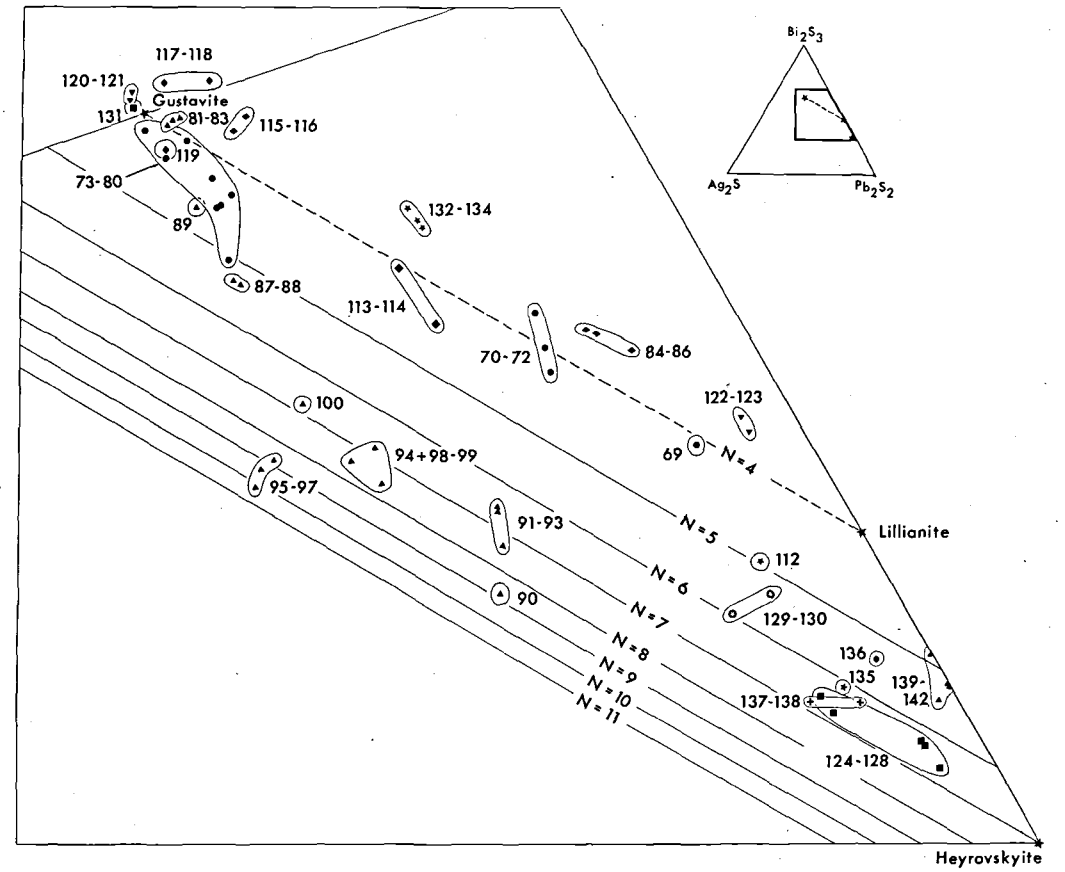

Fig. 7. Plot of the published chemical analyses listed in table 2. The numbers in the figure corresponds to analysis numbers at left column in table 2.

Polished section 36
$Ag_{1.42}Cu_{0.06}Pb_{2.34}Bi_{3.42}S_{8.18}$, N (chemical) = 6.18, L % = 67.9, x = 1.42 and Δx = 0.01.

The ideal formula is
$Ag_{1.50}Pb_{3.00}Bi_{3.50}S_9$, Z = 4, N (cryst.) = 7.0, L % = 60 % and x = 1.50.

The calculated density based on the ideal composition is 7.12 g/cm³.

Ourayite
Ourayite has been found only in specimen ROM M4100 labelled 'beegerite', Old Lout Mine, Ouray, Colorado, USA. The name is after the locality. The mineral was erroneously considered identical with schirmerite in the descriptions by the author (KM73b).

Ourayite occurs as irregularly shaped laths, less than 0.1 mm in length, enclosed in a very fine grained matrix of galena and matildite. The last two minerals were probably decomposition products of schapbachite. The optical properties of ourayite are indistinguishable from those of gustavite, vikingite and eskimoite. Due to the fine grain size of the mineral reflectance and microindentation hardness could not be recorded.

Single crystal examinations show that the ourayite is orthorhombic with a = 13.457(14) Å, b = 44.042(40) Å, c = 4.100(10) Å and space groups Bbmm or $Bb2_1m$. Crystallographic N = 11. Gandolfi powder data are listed in table 5.

Microprobe analyses of 11 grains (table 1, 8) are plotted in fig. 4, 8. The analyses suggest:

Table 4. X-ray powder data on eskimoite in polished section 35 (Gandolfi camera. Cu Kα-rad.)

I	^{d}hkl Meas.	^{d}hkl Calc.	Indices
3	3.53	3.53	270
10	3.36	3.37	$2\bar{8}0$
3	3.22	3.21	280
5	2.96	2.93	290
6	2.87	2.86	331
1	2.80	2.81	$2.\bar{1}0.0$
2	2.72	2.69	2.10.0
1	2.22		
4	2.08		
5	2.05		
2	1.776		
5	1.754		
4	1.667		
1	1.474		
1	1.448		
1	1.393		
3	1.328		
3	1.307		
2	1.292		
1	1.300		
1	1.212		
1	1.189		
1	1.179		
3	1.121		

Table 5. X-ray powder data on ourayite in spl. ROM M4100 (Gandolfi camera. Cu Kαrad.)

I	^{d}hkl Meas.	^{d}hkl Calc.	Indices
10	3.43	3.46	161
		3.44	2.11.0
6	3.33	3.35	410
		3.33	420
2	3.20	3.22	2.12.0
		3.19	181
2	3.05	3.03	2.13.0
9	2.96	3.00	321
		2.92	314
6	2.85	2.92	351
		2.85	2.14.0
1	2.17		
9	2.09		
7	2.04		
2	2.00		
1	1.97		
1	1.84		
7	1.79		
2	1.76		
2	1.73		
3	1.71		
4	1.66		
1	1.48		
2	1.36		
5	1.32		
3	1.29		
3	1.21		
2	1.18		

$Ag_{2.76}Cu_{0.19}Pb_{3.40}Bi_{4.76}S_{11.92}$, N (chemical) = 9.92, L % = 69.8, x = 2.76 and x = 0.01.
The ideal formulae is
$Ag_{12.5}Pb_{15}Bi_{20.5}S_{52}$, Z = 1, N(cryst.) = 11.0, L% = 69.4 and x = 3.125.

The calculated density using the ideal formula is 7.24 g/cm³.

Treasurite

Treasurite forms an 1 × 1.5 mm aggregate in sample R9714, labelled 'schirmerite'. The mineral is named after its locality, the Treasury Mine, Colorado, USA. The mineral was erroneously identified as schirmerite by KM73b.

The aggregate contains only a few treasurite grains. Partial, presumably hypogene, alteration of the mineral has resulted in the intergrowth of a very fine grained mineral with the same optical properties as treasurite. This secondary mineral is described below as 'the treasurite decomposition mineral.'

The optical properties of treasurite are indistinguishable from those of vikingite, eskimoite or ourayite. The fine grain size has excluded the determination of reflectance and microindentation hardness.

Weissenberg photographs show that treasurite is monoclinic: a = 13.349(10) Å, b = 26.538(20) Å, c = 4.092(7) Å, γ = 92.77(7)° and space groups B2/m, B2 or Bm. Gandolfi examination of the single crystal fragment gave a number of diffraction lines. Those indexed as treasurite powder lines are listed in table 6. Additional unindexable lines, considered to have resulted from mineral impurities in the examined fragment have been omitted from the table.

Crystallographic $N_1 = 4$, $N_2 = 8$ and $N_{average} = 6$.

Microprobe analyses on 5 treasurite grains are listed in table 1, 9 and plotted in fig. 4, 9. The analyses suggest
$Ag_{1.90}Pb_{1.50}Bi_{3.90}S_{8.33}$, N (chemical) = 6.33, L % = 87.8, x = 1.90 and Δx = 0.04.
The ideal formula is
$Ag_{1.75}Pb_{1.50}Bi_{3.75}S_8$, Z = 4, N (cryst.) = 6, L % = 87.5 and x = 1.75.

The calculated density using the ideal formula is 7.25 g/cm³.

Table 6. X-ray powder data on treasurite in spl. R9714 (Gandolfi camera. Cu-rad.)

I	d_{hkl} Meas.	d_{hkl} Calc.	Indices
5	3.63	3.60	260
10	3.49	3.56	131
3	3.35	3.36	270
8	3.22	3.23	270
1	3.18	3.20	420
5	2.93	2.91	280
5	2.86	2.88	331
5	2.82	2.82	331
3	2.09	2.09	551
		2.09	630
		2.08	640
	2.03	2.05	002
		2.04	012
6	1.989	2.02	660
		2.02	650
6	1.955	1.962	561
		1.958	670
		1.958	3.10.1
1	1.824	1.817	690
1	1.757	1.779	262
		1.767	0.15.0
2	1.732	1.734	690

Treasurite decomposition mineral

The treasurite decomposition mineral is very fine grained which excludes single crystal studies. Microprobe analyses on 8 grains are listed in table 1, 10 and plotted in fig. 4, 10. They suggest: $^{7.30}L_{87.5}$ with x = 2.32 and $\Delta x = 0.05$.

Schirmerite

Schirmerite in polished section 2571, previously described by Ramdohr (1955) and KM73b, is the most complex of the Ag-Pb-Bi sulphides so far discovered. The mineral occurs as lamellar crystals up to 2 mm in length interstitial to quartz. It is sometimes replaced by a very fine grained sulphide considered to be hypogene in origin. This mineral is described below as the 'schirmerite decomposition mineral'.

Microprobe analyses on 20 schirmerite grains are listed in table 1, 11–30 and plotted in fig. 4, 11–30. The analyses lie within a narrow, elongated field parallel to a line with nearly constant $Ag/\Sigma Me$. Three relatively large grains were each analyzed at several points (table 1, 31–33, fig. 4, 31–33). The analyses of the three grains suggest a relatively homogeneous composition of each grain.

A fragment giving the analysis no. 33 in table 1, was isolated for single crystal examinations. The Weissenberg photographs show that the schirmerite is strongly disordered (M-KM77b). The linear shape of the compositional field (fig. 4, 11–30) suggests that each grain is composed of two types of galena-like layers with different layer thickness. The composition field nearly extends between that of the pure end member gustavite (N = 4, $AgPbBi_3S_6$) and a point on the line with N = 7 corresponding to the composition $Ag_{1.5}Pb_3Bi_{3.5}S_9$. These two end members are thus considered to represent the composition of the two principal types of layers. Their presence in variable proportions explain the elongated composition field of schirmerite. Therefore, the conventional mineralogical properties such as cell dimensions, unit cell content, density, etc., cannot be assigned to schirmerite. However, each grain is characterized by distinct chemical N, substitution percentage (L %) and substitution factor (x). These values for each of the analyzed grains are given in table 1.

The optical properties of the individual schirmerite grains do not differ visibly, and the grains cannot be distinguished from other lillianite homologues by these properties.

Schirmerite decomposition mineral

This mineral is very fine-grained, excluding single crystal studies. Optically it cannot be distinguished from schirmerite. Microprobe analyses, completed on the mineral in two distinct aggregates (table 1, 34 and 35 plotted in fig. 4, 34 and 35) suggest

$^{8.57}L_{62.4}$ with x = 2.05 and $\Delta x = 0.16$ and

$^{9.06}L_{59.6}$ with x = 2.10 and $\Delta x = 0.06$.

Unnamed mineral($^{5.90}L_{65.7}$)

A lamellar-like mineral in specimen 1139 from Old Lout Mine, Colorado, USA, previously identified as gustavite (KM72) was too fine grained for single crystal studies. Microprobe analyses (table 1, 68, fig. 5, 68) suggest:

$^{5.90}L_{65.7}$ with x = 1.28 and $\Delta x = 0.01$.

Lillianite-gustavite solid solution series

A relatively large number of mineral varieties belonging to the lillianite-gustavite solid solution series have been identified (table 1, 36–47). Extensive solid solution in the series has been suggested for high temperatures (Hoda & Chang 1975). At lower temperatures the microprobe analyses and Weissenberg single crystal studies

suggest an imiscibility gap in the series between Gus≈50 and Gus≈85 (M-KM77b). According to the microprobe analyses the original Ivigtut high temperature gustavite has decomposed to $^{3\cdot77}$Gus$_{86.4}$ with exsolved submicroscopic blebs of $^{3\cdot82}$Gus$_{58.7}$ (KM70). Analyses 40 and 41 in table 1 and fig. 3 are reproduced from (KM70). The blebs are evenly distributed or locally concentrated in narrow zones, which appear as lamellae under the ore microscope. (See figures in KM70).

The microprobe analyses on the exsolved phase may therefore not represent its true composition. Weissenberg single crystal studies suggest the composition Gus$_{30.3\pm1.0}$ and Guinier powder data the composition Gus$_{24.9\pm1.0}$. Recently microprobe analyses were carried out on 6 grains in the type specimen (No 1973–188) containing very thin and evenly distributed lamellae. Each grain was analyzed in 15 different spots in order to determine the bulk composition of host and exsolved lamellae. The results (table 1, 39) suggest an original high temperature $^{3\cdot81}$Gus$_{75.1}$. Using the same approach analyses of the two varieties in polished section 58a suggest an original $^{3\cdot67}$Gus$_{74.7}$ in this section (table 1, 38). The average of the two is $^{3\cdot74}$Gus$_{74.9}$. The analyses are plotted in fig. 3.

Microprobe analyses on gustavite in sample 1139 from Old Lout mine in Colorado showed a compositional range of $^{3\cdot41}$Gus$_{116.1}$ to $^{3\cdot83}$Gus$_{79.6}$ (table 1, 48 to 66). Several of these gustavite grains are distinctly oversubstituted by Ag+Bi beyond Gus$_{100}$ up to Gus$_{116}$. Increasing substitution is accompanied by decreasing chemical N from 3.98 to 3.32. The analyzed grains may represent a submicroscopic intergrowth in all proportions of a copper-poor pavonite and a high temperature Gus≈80 (KM-M77).

One gustavite grain (composition not determined) in sample 1139 was extracted for single crystal studies. Two parallel oriented gustavite lattices similar to those from Ivigtut were identified suggesting that the bulk composition of the original high temperature phase lay within the same miscibility gap as the original Ivigtut high temperature gustavite.

Gustavites with end member composition were identified in samples 1140 ($^{3\cdot75}$Gus$_{103.0}$, table 1, 36 and fig. 5, 36) and 1124 ($^{3\cdot80}$Gus$_{100.1}$, table 1, 37 and fig. 6, 37).

Gustavites in the compositional range of Gus$_{80}$ – Gus$_{100}$ have been described by Nedachi, Takeuchi, Yamaoka & Taniguchi (1973), Harris & Chen (1975), Czamanske & Hall (1975), Borodaev & Mozgova (1971), Nuffield (1975) and KM72. See table 2 and fig. 7.

Members within the range Gus$_{12.5}$ to Gus$_{55}$ analyzed during the present study (table 1, 42 to 47) are plotted in fig. 4. Analyses within the same range have been published by Nedachi et al. (1973) and Klomínský, Rieder, Kieft & Mráz (1971). Cosalite(?) by Czamanske & Hall (1975) and 'Se-free and Ag-bearing wittite' by Ontoev, Troneva, Tsepin, Vyalsov & Basova (1972) may both represent members of the lillianite-gustavite series (table 2, 84–86 and 132–134, respectively).

No silver-free lillianites have yet been discovered and at present "bursaite" ($^{3\cdot82}$Gus$_{12.2}$, table 1, 47) represents the most silver-poor end member of the series analyzed. (The 'bursaite' material analyzed was borrowed from Dr. M. Rieder, Prague).

Cosalite

The ideal composition of cosalite ($Pb_2Bi_2S_5$) would suggest that the mineral is a lillianite homologue with N=3 (fig. 1). However, the crystal structure of cosalite shows that the mineral does not belong to the lillianite homologous series. Cosalite has been found in several of the parageneses investigated. Microprobe analyses are listed in table 8 and plotted in figs 3 and 4.

In the bottom part of table 8 the mol. values have been calculated on basis of the ideal unit cell content of sulphur which is 20 atoms. The corresponding sum of metals (right column in the table) lies between 15.77 and 17.28.

Srikrishnan & Nowacki (1974) found close to one copper atom per unit cell which occurs statistically in the structure, coordinated tetrahedrally with sulphur. The content of metals in the unit cell of the mineral would then reach 17. The two analyzed cosalites from Ivigtut appear to represent cosalite with maximum Me^+ contents known.

The microprobe analyses plotted in figs 8A and 8B show that the presence of copper and/or silver in the structure of the mineral is mainly accompanied by the removal of lead according

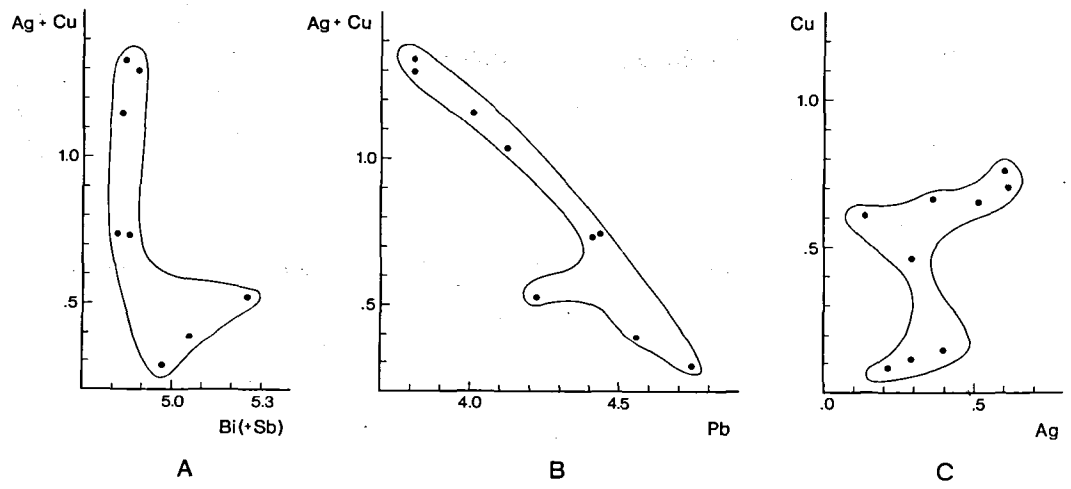

Fig. 8. Plots of cosalite microprobe analyses (table 8) showing relationships in mol. values between (Ag+Cu) and Bi (A), (Ag+Cu) and Pb (B) and between Ag and Cu (C). Sum of Ag+Cu+Pb+Bi+Sb = 10.0.

presumably to the following substitutional scheme: $Pb^{++} \leftrightarrow 2(Ag,Cu)^{+}$. One Me^{+} atom (preferencially copper ?) would then take the tetrahedral position and the other the position of the substituted Pb^{++}. At the same time the substitutional scheme $2Bi^{+++}$ for $3Pb^{++}$ leaving one Pb^{++} position emty (Otto & Strunz 1968) might also take place. This may explain the relatively bismuth-rich cosalites from Japan (fig. 4, C9).

Fig. 8C suggests that no obvious relationships exist between copper and silver in cosalite. However, silver-rich cosalites in general have relatively high contents of copper. For instance, the Ivigtut cosalites contain around 3 % silver and 2 % copper. Presumably cosalite with high silver contents cannot be stable unless copper is present. Instead of the cosalites, a member of the gustavite-lillianite series would form. It is assumed, that the major reason for cosalite to form associasions with a gustavite-lillianite member is the presence of small amounts of copper which apparently cannot be accommodated in the structure of lillianite homologues.

Description of Mineral Parageneses

1. The gustavite-cosalite-galena paragenesis from the cryolite deposit, Ivigtut, South Greenland

Gustavite, vikingite, eskimoite, cosalite, galena, aikinite and berryite form the bulk of this paragenesis. The composition of the first four minerals are plotted in fig. 3. The microprobe analyses show that cosalite (fig. 3, C1 and C2) associated with vikingite contains more silver than those (fig. 3, C3 and C4) associated with gustavite, but similar amounts of copper.

Microprobe analyses on berryite (table 11, 1) gave nearly the same atomic ratios as the original microprobe analyses on this mineral (KM66). Microprobe analyses on aikinite (table 10A) gave nearly ideal aikinite composition. Microprobe analyses on galena in two polished sections are listed in table 7 and show a distinct surplus of bismuth over silver (mol. values).

$^{3}\cdot^{77}Gus_{86.4}$, containing exsolved, visible lamellae of $^{3}\cdot^{82}Gus_{58.7}$, can be distinguished from vi-

Table 7: Microprobe analyses for Ag and Bi in galena. A: 4 grains in polished section 2954 (Agenosawa mine, Japan), B: 7 grains in polished section LS-70-B4-1 (Is Lassinus, Sardinia, Italy), C: 8 grains in polished section 2568 and polished section 2569 (Kingsgate, NSW, Australia), D: 10 grains in polished section 3 (Ivigtut), E: 11 grains in polished section 36 (Ivigtut) and F-1 to F-8: spot analyses across the galena band in spl. 1139 (Colorado, USA).

	Ag		Bi		Ag Atomic ratio	Bi Atomic ratio	Pb Atomic ratio	Ag:Bi Atomic ratio
	Wt.%	esd	Wt.%	esd				
A	0.92	0.06	2.97	0.34	2.02	3.37	94.61	.60
B	0.60	0.05	1.77	0.28	1.32	2.02	96.67	.65
C	0.14	0.09	2.01	0.74	0.31	2.30	97.39	.13
D	1.4	–	3.3	–	3.07	3.73	93.21	.82
E	2.08	0.17	5.44	0.41	4.52	6.10	89.39	.74
F–1	0.14	–	0.26	–	0.31	0.30	99.40	1.05
–2	0.48	–	1.25	–	1.06	1.42	97.52	.74
–3	0.91	–	1.89	–	2.00	2.14	95.86	.93
–4	1.14	–	2.21	–	2.50	2.50	95.00	1.00
–5	1.29	–	2.60	–	2.82	2.94	94.24	.96
–6	2.52	–	5.61	–	5.45	6.26	88.30	.87
–7	2.71	–	5.15	–	5.84	5.73	88.42	1.02
–8	3.34	–	7.01	–	7.16	7.75	85.09	.92

kingite and eskimoite only in polished sections etched with conc. HNO_3. When $^{3.82}Gus_{58.7}$ is submicroscopically present optical distinction between the three minerals is not possible. The existence of vikingite and eskimoite was therefore not recognized by KM73a.

Vikingite has been positively identified in three polished sections and displays similar relationships as gustavite towards cosalite and galena.

Eskimoite has been positively identified in two polished sections where it is developed as host for abundant berryite, aikinite and galena (KM66). Consequently in all berryite- and aikinite-rich samples eskimoite might be the host. Since cosalite has never been found in any of these, cosalite may not occur intergrown with eskimoite, only with gustavite and vikingite.

2. Specimen 1139, Old Lout Mine, Colorado, USA

This sample is composed of a 1 cm thick sulphide band in gangue (KM72). The band is composed of three layers.

The bismuthinite-benjaminite-pavonite-gustavite-layer forms the bulk of the sulphide band and is composed of up to 0.5 mm large bismuthinite grains embedded in a matrix of benjaminite, pavonite and gustavite disseminated with very fine grained bismuthinite and tetrahedrite. No minerals are enclosed in the large bismuthinite grains. Benjaminite cannot be distinguished optically from pavonite and only pavonite was recognized in the earlier study of the sample (KM72). During the present investigation the two sulphides were distinguished by means of detailed microprobe analyses followed up by single crystal investigation (Weissenberg method) on analyzed grains. The benjaminite crystal fragment contained a small proportion of submicroscopic gustavite (KM-M77). The microprobe analyses on pavonite and benjaminite are plotted in fig. 5, C and D, respectively. Pavonite was found near the large bismuthinite grains, and benjaminite at a greater distance from these in more gustavite-rich environments.

With increasing distance from the large bismuthinite grains the amount of gustavite increases and is locally the only mineral present. A marked change in its composition across the layer was recorded. It is richest in silver and bismuth closest to the large bismuthinite grains. The composition of 19 analyzed grains (table 1, 48–66) are plotted in fig. 5, 48–66, and discussed above.

The fine grained disseminated bismuthinite was not analyzed by the microscope. The composition of the large grain is given in table 9, A.

The layer characterized by $^{5.90}L_{65.7}$ lies in sharp contact with gustavite. Across the layer increasing amounts of galena occur interstitial to the $^{5.90}L_{65.7}$ lamellae and finally a gradual change into the following galena layer takes

Table 8. Microprobe analyses on cosalite. C1: 7 grains in polished section 2 (Ivigtut), C2: 8 grains in polished section 31 (Ivigtut), C3: 7 grains in polished section 1973–188 (Ivigtut), C4: 11 grains in polished section 58 a (Ivigtut), C5: 9 grains associated with galenobismutite in polished section 2569 (Kingsgate, Australia), C6: 6 grains associated with $^{3\cdot75}Gus_{40.2}$ in polished section 2568 (Kingsgate, Australia), C7: analysis on one grain in polished section LS-70-B4-1 (Is Lassinus, Sardinia, Italy). C8: 7 grains in polished section 2550 (McElroy, Township). C9: 10 grains in polished section 2953 (Agenosawa mine, Japan).

	Ag		Cu		Pb		Bi		Sb		S		
	Wt.%	esd	Wt.%	esd	Wt.%	esd	Wt.%	esd	Wt.%	esd	Wt.%	esd	Total
C1	3.0	0.1	2.0	0.1	35.2	0.2	45.4	0.2	–	–	16.5	0.1	102.1
C2	2.8	0.2	2.1	0.1	35.0	0.5	44.9	0.4	–	–	16.5	0.2	101.3
C3	2.4	0.3	1.8	0.1	35.7	0.5	43.5	0.3	–	–	16.3	0.1	98.7
C4	1.7	0.3	1.8	0.2	37.0	0.9	43.9	0.9	–	–	16.7	0.3	101.1
C5	1.2	0.1	0.3	0.1	38.6	0.7	41.3	0.5	1.2	0.1	16.6	0.6	99.2
C6	1.0	0.1	0.2	0.1	40.7	0.7	41.7	1.9	0.8	0.2	16.2	0.2	100.6
C7	1.3	0.1	1.2	0.1	38.8	0.2	42.5	0.3	–	–	16.3	0.5	100.1
C8	0.6	0.6	1.7	0.1	38.9	0.2	43.2	0.7	–	–	16.8	0.1	101.2
C9	1.7	0.1	0.4	0.1	35.9	0.6	45.0	0.4	–	–	16.2	0.5	99.2
Atomic ratios													Sum of metals
C1	1.06		1.21		6.59		8.42		–		20.0		17.28
C2	1.02		1.30		6.57		8.34		–		20.0		17.23
C3	0.86		1.10		6.77		8.16		–		20.0		16.89
C4	0.61		1.12		6.88		8.09		–		20.0		16.70
C5	0.43		0.18		7.19		7.61		0.36		20.0		15.77
C6	0.35		0.12		7.70		7.90		0.25		20.0		16.32
C7	0.48		0.77		7.37		7.99		–		20.0		16.61
C8	0.20		1.00		7.19		7.91		–		20.0		16.30
C9	0.64		0.23		6.86		8.53		–		20.0		16.26

place (fig. 6 in KM72). Variable amounts of tetrahedrite in patchy aggregates are enclosed in the $^{5\cdot90}L_{65.7}$ layer.

Microprobe analyses across *the galena layer* display a significant change in the silver and bismuth content of the galena from high towards low values away from $^{5\cdot90}L_{65.7}$ (table 7, F-1 to F-8, see also fig. 10). The molar ratio of silver and bismuth dissolved in the galena is close to one in each of the analyzed spots.

3. Bi-Pb-(Ag-Cu) sulphides from Kingsgate, Australia

A number of Pb-Bi sulphides from the molybdenite occurrences at Kingsgate (Yarrow Creek) in NSW, Australia, have been described by Lawrence and Markmann (1962). These sulphides occur together with a number of Bi-tellurides mainly in association with pyrrhotite-chalcopyrite mineralizations.

In 1962 Professor P. Ramdohr gave the author two sulphide samples from Kingsgate. In one of these (polished section 2569) aggregates isolated in gangue are composed of galenobismutite intimately intergrown with bismuthinite. The relationships between the two sulphides suggest penecontemporaneuos crystallization. Monomineralic aggregates of cosalite were also present.

Microprobe analyses on cosalite are listed in table 8, C5 and plotted in fig. 4, C5, and those for bismuthinite are listed in table 9, E. Microprobe analyses on 4 galenobismutite grains gave the composition: Pb = 27.0±0.3 %, Bi = 56.1±0.2 %, Sb = 0.4±0.1 % and S = 17.0±0.4 % summing at 100.5 % and suggesting the formula $Pb_{1.00}Bi_{2.05}S_{4.00}$, which is close to that of ideal galenobismutite ($PbBi_2S_4$). Silver and copper were not present in detectable amounts.

In the other sample (polished section 2568), aggregates are composed of cosalite, $^{3\cdot75}Gus_{40.2}$ and galena. In general galena is present only in small amounts but may locally dominate. It then appears as host for the two other sulphides and appears to have crystallized later than these. Numerous inclusions of very fine grained galena may occur enclosed in cosalite. Rarely, graphic intergrowth between the two minerals has been observed, indicating penecontemporaneous crystallization.

Microprobe analyses on $^{3\cdot75}Gus_{40.2}$ are listed in table 1, 44 and plotted in fig. 4, 44. Those on

Table 9. Microprobe analyses for minor elements in A: 8 bismuthinite grains associated with pavonite in spl. 1139, B: 8 grains of bismuthinite associated with pavonite (?) in spl. ROM M21003, C: 12 grains of bismuthinite associated with pavonite in spl. BSF 1821, D: 5 grains of bismuthinite associated with $^{3.75}Gus_{103.0}$ and pavonite in spl. 1440 and E: 7 grains of bismuthinite associated with galenobismutite in polished section 2569 (Kingsgate, Australia).

	Ag		Cu		Pb		Sb	
	Wt.%	esd	Wt.%	esd	Wt.%	esd	Wt.%	esd
A	–	–	0.26	0.11	1.04	0.16	3.15	0.89
B	0.05	0.04	0.24	0.05	0.54	0.17	0.13	0.06
C	0.02	–	0.39	0.05	1.56	0.11	2.15	0.29
D	0.06	0.03	0.21	0.03	0.32	0.21	2.03	0.19
E	0.01	–	0.44	0.07	1.57	0.18	0.24	0.17

cosalite are listed in table 8, C6 and plotted in fig. 4, C6. In table 7 the probe analyses on galena are given. The sample has contributed the following mineral association to those given from Kingsgate by Lawrence & Markmann (1962): galena-cosalite-$^{3.75}Gus_{40.2}$.

4. Ag-Pb-Bi sulphides from the Agenosawa Mine, Japan

Three mineral varieties, Gustavite ($Gus_{>80}$), phase X ($Gus_{\approx 44.0}$) and phase Z ($Gus_{24.0}$), apparently belonging to the lillianite-gustavite series (table 2), were found in the sulphide mineralizations from the Agenosawa Mine (Nedachi et al. 1973). The following mineral associations were recognized: bismuthinite-cosalite (A), cosalite-phase Z-galena (B), bismuthinite-phase X-gustavite (C) and bismuthinite-pavonite-gustavite (D). A general shift in the crystallization of the associations took place in the direction A → B → C → D. Temperatures of formation were assumed to be lower than 250°C.

During the present study a specimen from the Agenosawa mine was obtained from Dr. Kato (Tokyo). It was composed of massive pyrrhotite enclosing bladed aggregates of Ag-Pb-Bi sulphides dominated by bismuthinite. The following associations were identified:

(1) bismuthinite-cosalite-$^{3.85}Gus_{51.0}$ and
(2) bismuthinite-cosalite-$^{3.89}$ $Gus_{29.1}$-galena.

In association (1) large grains of bismuthinite are separated from the enclosing pyrrhotite by a layer of cosalite crystals which are idiomorphic against the bismuthinite. Near the margin towards pyrrhotite, cosalite is intergrown with $^{3.85}Gus_{51.0}$. Microprobe analyses on cosalite are listed in table 8, C9 and those for $^{3.85}Gus_{51.0}$ in table 1, 43. The analyses are plotted in fig. 4, 43 and C9.

In association (2) large bismuthinite grains similar to those in (1) are surrounded by cosalite. However, at one place the cosalite layer abruptly changes into a heterogeneous mixture of pyrrhotite and galena containing lamellae of $^{3.89}Gus_{29.1}$. Microprobe analyses on galena are listed in table 7, A and those on $^{3.89}Gus_{29.1}$ in table 1, 45. The latter analysis is plotted in fig. 4, 45.

The crystallization sequence in association (1) is: pyrrhotite → cosalite + $^{3.85}Gus_{51.0}$ → cosalite → bismuthinite. In (2) a break in the crystallization sequence appears to have taken place. At first $^{3.89}Gus_{29.1}$ crystallized as lamellae in galena, hence the sequence: $^{3.89}Gus_{29.1}$ → galena. Then follows the sequence cosalite → bismuthinite, as in association (1) after the apparent break.

5. Ag-Cu-Pb-Bi mineralization from Is Lassinus, Sardinia, Italy

Dr. E. A. J. Burke, Amsterdam, kindly contributed two polished sections of mainly chalcopyrite in gangue from an abandoned Pb-Zn mine at Is Lassinus. This locality is situated about 500 m southeast of Monte Tamara near the village Nuxis in the Sulcis district, Southern Sardinia, Italy. The ore occured in a recrystallized limestone of Cambrian age. A number of sulphides were identified in two polished sections. Chalcopyrite, magnetite and sphalerite dominates. Accessory sulphides enclosed mainly in the chalcopyrite are: carrollite, cobaltite, wittichinite, hammarite, $^{3.66}Gus_{55.8}$, cosalite and galena.

Carrollite and cobaltite are irregularly inter-

grown with each other and occur in the major sulphides without being associated with any of the other accessory sulphides. Microprobe analyses, completed by Dr. Kieft (personal communication), gave the following composition of the two minerals: carrollite: $Co_{2.16}$ $Ni_{0.29}$ $Fe_{0.06}Cu_{0.47}$ $S_{4.00}$; cobaltite: $Co_{0.87}$ $Fe_{0.07}$ $Ni_{0.02}$ $As_{1.00}$ $S_{1.03}$.

$^{3.66}Gus_{55.8}$ and hammarite are closely associated. The former is shaped as rectangular grains, the latter as equidimensional grains. Microprobe analyses on $^{3.66}Gus_{55.8}$ are listed in table 1, 42 and plotted in fig. 4, 42. The two microprobe analyses on the mineral by Dr. Kieft are given in table 2, 113 and 114. They are plotted in fig. 7, 113 and 114. Analyses on associated hammarite are listed in table 10. D. Sometimes galena in graphic intergrowth with hammarite is enclosed between $^{3.66}Gus_{55.8}$ grains. Often a galena replacement rim separates the two minerals but it appears to be of the same age as the hammarite-galena intergrowth. The galena in this association was too fine grained to permit microprobe analyses to be carried out.

Wittichinite rarely occurs associated with $^{3.66}Gus_{55.8}$, hammarite and galena. The microprobe analysis on wittichinite by Dr. Kieft gave the composition: $Cu_{2.84}$ $Ag_{0.11}$ $Fe_{0.06}$ $Pb_{0.03}$ $Bi_{1.01}$ $S_{2.95}$.

Laths of $^{3.66}Gus_{55.8}$ may lie isolated in chalcopyrite sometimes separated from this mineral by the late galena rim.

One relatively large cosalite grain (table 8, C7 and fig. 4, C7) with enclosed lamellae of hammarite (table 10, E) has been identified.

6. Pb-Bi-Ag sulphides from theYakuki mine, Fukushima, Pref., Japan

Heyrovskyite, first described by Klomínský et al. (1971), has recently been found at the Yakuki mine in Japan. Dr. Kato kindly contributed a specimen from this locality.

Polished section 2801 contains two small sulphide aggregates. Heyrovskyite ($^{6.68}Hey_{9.6}$) is present as equidimensional to lamellar, randomly oriented grains. In one of the aggregates $^{3.86}Gus_{21.0}$ occurs in amounts of about 10 %. The mineral is shaped as lamellae and it is often impossible optically to distinguish between the two minerals. Microprobe analyses on $^{3.86}Gus_{21.0}$ are listed in table 1, 46 and they are plotted in fig. 4, 46. Those on heyrovskyite is given in table 1, 67 and they are plotted in fig. 4, 67.

7. Specimen 1124. Alaska Mine, Colorado, USA

The specimen is composed of pavonite with small amounts of interstitial gustavite. The pavonite contains an exsolved pavonite variety (KM-M77). The analyses on two pavonite grains are plotted as H and I in fig. 6 and those on the exsolved variety in these two grains as K and J, respectively. The composition of associated gustavite (table 1, 37) is also plotted in fig. 6, 37 and

Table 10. Microprobe analyses on members of the bismuthinite-aikinite group of minerals. A: average of 10 grains analyzed in spl. 36 (Ivigtut). B: 7 grains in spl. ROM M13805, C: 5 grains in spl. ROM M21003, D: 2 grains associated with $^{3.66}Gus_{55.8}$ in polished section LS-70-B4-1 (Is Lassinus, Sardinia, Italy) and E: 3 grains enclosed in cosalite grains in polished section LS-70-B4-1, F: 2 grains in polished section 2550 (McElroy, Township, Ontario, Canada).

	Ag	Cu		Pb		Bi		Sb		S		
	Wt.%	Wt.%	esd	Wt.%	esd	Wt.%	esd	Wt.%	esd	Wt.%	esd	Total
A	0.1	10.2	0.1	33.9	0.5	39.5	1.2	–	–	17.0	0.3	100.7
B	–	8.0	0.1	26.1	0.5	47.2	0.7	–	–	17.3	0.1	98.6
C	–	6.4	0.2	21.4	0.9	57.2	0.8	0.2	0.1	17.1	0.6	102.3
D	–	7.9	0.3	26.5	1.4	48.3	0.7	–	–	17.9	0.1	100.6
E	–	8.4	0.5	28.3	0.9	45.9	0.7	–	–	17.8	0.9	100.4
F	–	6.1	–	20.2	–	56.1	–	–	–	18.1	–	100.5
Atomic ratios:												
A	0.01	0.91		0.93		1.07		–		3.00		
B	–	0.70		0.70		1.26		–		3.00		
C	–	0.56		0.58		1.54		–		3.00		
D	–	0.72		0.74		1.19		–		3.00		
E	–	0.67		0.69		1.24		–		3.00		
F	–	0.51		0.52		1.43		–		3.00		

suggest a $^{3\cdot80}Gus_{100.1}$ – variety, i.e. an ideal gustavite.

8. Specimen 1140.
Gladiator Mine, Colorado, USA

Aggregates of Ag-Pb-Bi-Cu sulphides in quartz and pyrite displayed the following crystallization sequence: bismuthinite → pavonite → gustavite. Microprobe analyses on pavonite (KM-M77) are plotted in fig. 5, E. Those on gustavite (table 1, 36, fig. 5, 36) suggest a $^{3\cdot75}Gus_{103.0}$-variety. The microprobe analyses on bismuthinite are given in table 9, D.

9. Specimen BSF 1821.
Silver Bell Mine, Colorado, USA

This sample is composed of a bismuthinite-pavonite-rich layer in contact with a pavonite-gustavite-rich layer (KM72). The composition of pavonite (KM-M77) in the two associations is plotted in fig. 6 as B and A, respectively. The content of minor elements in the bismuthinite is given in table 9, C. Two microprobe analyses by KM72 on the gustavite gave: $^{3\cdot70}Gus_{104.8}$. (Table 2, 120 and 121, fig. 7, 120 and 121).

10. Specimen ROM M21003. Bolivar Mine,
Cerro Bonete, Lipez province, Bolivia

This specimen is composed of pavonite enclosing both bismuthinite (composition in table 9, B) and a member of the bismuthinite-aikinite series close to krupkaite in composition (table 10, C). A very fine grained, unidentified mineral has exsolved from the pavonite (KM72, fig. 4). Single crystal studies on the assumed pavonite were not possible due to the fine grain size and polysynthetic twinning of the mineral. The microprobe analyses (KM-M77) on the sulphide are plotted as F in fig. 6.

11. Specimen ROM M13805.
Manhattan, Nevada, USA

This specimen contains benjaminite with submicroscopic gustavite. Microprobe analyses on both phases (KM-M77) are plotted as G in fig. 6. The composition of enclosed berryite lamellae in benjaminite are given in table 11, B. A member of the bismuthinite-aikinite series with a composition near to that of krupkaite (table 10, B) lies in contact with the benjaminite.

Table 11. Microprobe analyses on berryite. A: 9 grains in polished section 36 (Ivigtut), B: 9 grains in spl. ROM M13805.

	A			B		
	Wt.%	esd	Atomic ratio	Wt.%	esd	Atomic ratio
Pb	21.6	0.8	12.8	19.5	0.4	11.8
Bi	48.9	1.4	28.1	48.3	0.6	30.0
Ag	6.8	0.1	7.6	6.7	0.2	7.8
Cu	6.1	0.1	11.5	5.8	0.1	11.4
S	17.2	0.3	64.4	17.3	0.1	67.5
Total	100.5			97.6		

12. PS 2550. McElroy, Township,
Ontario, Canada

Granular cosalite (table 8, C8) occurs as host for a mineral with close to krupkaite in composition (table 10, F).

Discussion

Silver- and bismuth-bearing galena

Amount of silver and bismuth dissolved in galena. Above 215±15°C complete solid solution exists between galena and matildite (Craig 1967). Synthetic galena at 175°C may contain up to about 10 mol. % dissolved $AgBiS_2$ (Van Hook 1960). The amount of silver and bismuth in the structure of natural galena retained at room temperatures varies considerably. The common Ivigtut galena found throughout the cryolite deposit contains up to 4 mol.% $AgBiS_2$ (Karup-Møller & Pauly in press). Galena with up to 7 mol.% $AgBiS_2$ has been described by Ontoev, Nissenbaum & Organova (1960) and also in this paper (table 7). High contents of the two metals in Se-bearing galena have been reported by Czamanske & Hall (1975). Exsolved matildite has not been found in any of the above cited galenas in spite of their frequently high contents of silver and bismuth.

However, galena from the Ivigtut galena-aikinite-matildite paragenesis (Karup-Møller & Pauly, in press) contains exsolved matildite. The original matildite content ranged from about 2 to 7 mol.%. After the matildite exsolution the dissolved content is only 2–3.5 %.

According to Van Hook (1960) galena may contain silver only in slight excess over bismuth even at high temperatures, while it may contain

considerably more bismuth than silver (e.g. table 7). Bismuth-free galena may contain up to 0.4 wt. % silver (Van Hook 1960, Salanci & Moh 1969, Leutwein & Hermann 1954) while silver-free galena may contain more than 10 wt.% bismuth. (Large & Mumme 1975).

The Ag-Bi ratio of the common Ivigtut galena, based on microprobe analyses, is 0.955 and that for galena in the Ivigtut galena-aikinite-matildite paragenesis is 1.029. Galena found in bismuth-rich mineral parageneses nearly always contains more bismuth than silver (table 7). Exsolved minerals have not been found in any of the galenas listed in table 7 in spite of the often large surplus of bismuth.

Position of Ag and Bi in the galena structure. Silver and bismuth substituting for lead ($Ag^+ + Bi^{+++} \leftrightarrow 2Pb^{++}$) in the galena structure occupy the substituted lead positions. Any surplus of silver over bismuth would, in order to maintain charge balance, require the entrance into the structure of 2 Ag^+ for each Pb^{++} removed. One of the two silver atoms would therefore have to be placed in interstitial positions in the galena structure. However, such positions are apparently not available, explaining why galena with more than a few tenths of a mol. percent silver in excess of bismuth has not been found in nature. On the other hand, surplus of bismuth is easily explained. For every three Pb^{++} removed, two Bi^{+++} enter into the galena structure ($3Pb^{++} \leftrightarrow 2Bi^{+++}$) resulting in one lead position being left empty. This conventional way of explaining the bismuth surplus may not be correct, especially in galenas with significantly more bismuth than silver. In these varieties it is possible that domains of the structure are similar to those of lillianite homologues. These domains would then consist of layers of the original galena structure twinned on (131) with lead atoms in trigonal prismatic coordination positioned in the twinning plane. The galena layers would have a considerable thickness corresponding to a high crystallographic N (compare M-KM77a). The layer thickness may not necessarily remain constant from one domain to another.

On the role of copper in the galena structure. During the present study special care has been exsercized in determining the content of copper in the silver- and bismuth-bearing galenas, especially those intergrown with copper-bearing minerals such as cosalite, aikinite, berryite and others. In no case has copper been found in amounts reaching 0.1 wt.%, although a distinct surplus of bismuth over silver occurs in several of the analyzed galenas.

Mineral associations

The term 'mineral association' is used in the following to represent an assemblage of two or more intimately intergrown sulphide minerals. The bulk of the sulphides forming an association in most cases is believed to have crystallized penecontemporaneously, presumably under conditions of equilibrium. However, often one of the minerals may also have crystallized somewhat earlier or later than the others. Some of the observed associations are characterized by a gradual shift during the crystallization from one mineral to another. Crystallization trends (next chapter) have thus been recognized in many of the studied polished sections. A polished section, e.g. PS 1139, may contain several separate associations and sharp distinction between these may be difficult.

The system Ag_2S-Pb_2S_2-Bi_2S_3 is divided into two subsystems by the galena-matildite join. The subsystem Ag_2S-Pb_2S_2-$AgBiS_2$ is of no interest here as no ternary compounds are known within it. In the other subsystem (Pb_2S_2-$AgBiS_2$-Bi_2S_3) a number of mineral associations were observed. They are listed in table 12. According to the typical assemblages the subsystem can be divided into the areas A-D in fig. 9.

Area A. Experimental studies (Hoda & Chang 1975) suggest the existence of the three assemblages: pavonite-bismuthinite, pavonite-gustavite and pavonite-matildite. Benjaminite has not been identified in the materials synthetized by these workers.

Nedachi et al. (1973) have identified the following two associations: pavonite-bismuthinite and pavonite-gustavite. The association benjaminite-matildite was described by Harris & Chen (1975).

During the present study (also KM72) the first 6 associations in table 12 (except the association benjaminite-matildite) were observed in one or several of the sulphide specimens from mineral

Table 12. Natural mineral associations in the Pb_2S_2-$AgBiS_2$-Bi_2S_3 subsystem. GL stands for members of the gustavite-lillianite series and LHS for the lillianite homologous series.

Area A in fig. 9
- Benjaminite – gustavite
- Benjaminite – matildite
- Benjaminite – bismuthinite
- Benjaminite – pavonite
- Pavonite – gustavite
- Pavonite – bismuthinite
- Pavonite – matildite

Area B in fig. 9
- Bismuthinite – galenobismutite
- Cosalite – bismuthinite
- Cosalite – galenobismutite
- Cosalite – galena
- Cosalite – bismuthinite - galenobismutite
- Galena – galenobismutite

Area C in fig. 9
- GL – cosalite
- GL – bismuthinite
- GL – galenobismutite

Area D in fig. 9
- GL – Ag-heyrovskyite
- GL – vikingite
- GL – eskimoite
- GL – $^{5-90}L_{65-7}$
- GL – cosalite
- Vikingite – cosalite
- Ag-Bi-galena (also schapbachite) – nearly all LHS members
- Ag-Bi-galena – cosalite

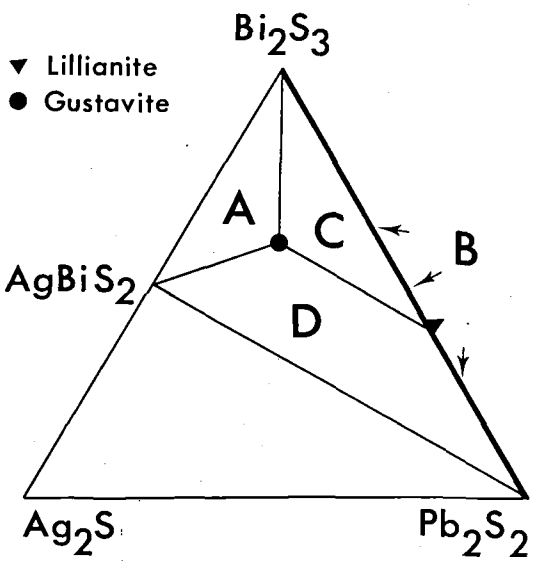

Fig. 9. Schematic subdivision of Pb_2S_2-$AgBiS_2$-Bi_2S_3 subsystem according to typical assemblages. For details see part 'mineral associations' in text.

deposits in Colorado (spls. 1124, 1139, 1140 and BSF 1821). All associations are characterized by small contents of Cu.

So far pavonite and benjaminite have only been found in association with gustavite, but they might also be able to crystallize in association with Ag-Bi end members of other lillianite homologue series with N greater than 4.

Area B. The relationships in this part of the subsystem are complicated by the presence of both cosalite and galenobismutite (cannizzarite with a composition assumed to lie between that of ideal cosalite and galenobismutite is very rare and has therefore been omitted). The following mineral associations are known: cosalite-galena, cosalite-galenobismutite, cosalite-bismuthinite, bismuthinite-galenobismutite and cosalite-galenobismutite-bismuthinite (e.g. Kingsgate, Australia). The association galena-galenobismutite has been reported by Goodell (1975).

Craig (1967) and Salanchi & Moh (1969) were not successful in synthesizing cosalite and they therefore assumed that the mineral is stable only at relatively low temperatures. This is substantiated by the decomposition of phases (often unknown) into graphic intergrowths of galena and cosalite (Ramdohr 1955; Klomínský et al. 1971; Craig 1967 and Mozgova et al. 1976). It is furthermore speculated that cosalite may only form in the presence of copper or silver or both (Craig 1967). All microprobe analyses on cosalite listed in table 8, show significant amounts of both elements.

The microprobe analyses on galenobismutite from Kingsgate failed to disclose the presence of silver and copper, although the mineral occurs in the same polished section as the silver- and copper-bearing cosalite. The small amounts of copper and silver may have caused the formation of cosalite and may thus explain the mineral association: cosalite-galenobismutite-bismuthinite described by Lawrence & Markmann (1962). In the pure ternary Pb-Bi-S system the coexistence of these three minerals appears impossible.

The association Ag-free heyrovskyite – Ag-free lillianite, known from experimental studies (e.g. phase II – phase III by Salanchi & Moh 1969) has not yet been observed in nature.

Giessenite has a composition very close to that of lillianite. The mineral is known from two

localities (Graeser 1963, Karup-Møller 1973c). The mineral from both localities contains small amounts of Sb, about 4 % Sb. This suggests that Sb-free giessenite may not form and that the mineral therefore may not belong to the Ag-(Cu)-Pb-Bi-S system.

Area C. The mineral association cosalite and a member of the lillianite-gustavite series from Kingsgate and Ivigtut and the association cosalite-bismuthinite-$^{3\cdot85}$Gus$_{51.0}$ from the Agenosawa mine fall within this area.

The association galenobismutite-lillianite reported by Kupčík et al. (1969) consisted of individual crystals in quartz. The relationships between the two sulphides in polished sections were not studied. An emission spectral analysis showed the presence of silver in the lillianite variety, but the amount was not determined. The cell dimensions published by Kupčík et al. (1969) suggest the composition Gus$_{12.5}$ (M-KM77b).

The discovery of the Agenosawa Ag-Bi-Pb-sulphides (Nedachi et al. 1973) has shown that it is most likely that the only mineral associations found in the middle and left part of area C consist of bismuthinite and members of the gustavite-lillianite series.

Area D. This part of the subsystem, bound by the gustavite-lillianite and galena-matildite series, is complex due to the existence of the numerous lillianite homologues.

The lillianite-gustavite series is rather densely populated with naturally occurring varieties, which suggests that they are the most easily formed. They also are the only Ag-bearing lillianite homologues reported from experimental studies (Hoda & Chang 1975). It is therefore assumed that bismuthinite and galenobismutite may not coexist with lillianite homologues except those belonging to the lillianite-gustavite series.

The coexistence of different lillianite homologues has been observed. $^{3\cdot86}$Gus$_{21.0}$ occurs as laths in heyrovskyite ($^{6\cdot68}$Hey$_{9.6}$) from the Yakuki mine in Japan (fig. 4). At Ivigtut, $^{3\cdot74}$Gus$_{74.9}$, vikingite and/or eskimoite might coexist but due to nearly identical optical properties distinction between them in the polished section was not possible. In polished section 1139 (Old Lout Mine, Colorado) the association $\approx$ $^{3\cdot9}$Gus $\approx$ $_{80.0}$ – $^{5\cdot90}$L$_{65.7}$ was identified.

The association between lillianite homologues and Ag-Bi-rich galenas has been observed at many deposits (fig. 10).

Although Hoda & Chang (1975) on basis of their experimental studies suggest simple relationships in the system, natural lillianite homologues may coexist yielding a large number of mineral associations. Characteristic is the association of many lillianite homologues with silver- bismuth-rich galena. Another characteristic feature is the crystallization of cosalite in association with a lillianite homologue when small amounts of copper are present. Higher copper contents may result in the formation of for instance, berryite, or aikinite instead of cosalite (Ivigtut).

The composition of cosalite varies accordingly. Ag-Cu free cosalite fall within area B, Ag-Cu-poor cosalites within area C and Ag-Cu-rich varities within area D. Thus at Ivigtut cosalite has been found in association with vikingite and this cosalite variety apparently represents the most silver- and copper-rich variety so far discovered.

Crystallization sequences

The estimated crystallization sequences recognized in the studied materials are plotted in fig. 10. In the upper left and central part of the Ag-(Cu)-Pb-Bi-S system the mineral relationships in samples 1140 and in the materials from the Agenosawa mine described by Nedachi et al. (1973) suggest the following crystallization sequence: Bismuthinite → pavonite → gustavite. Nedachi et al. (1973) also described the sequence: bismuthinite → gustavite or an Ag-Bi-rich member of the lillianite-gustavite series. By analogy with the crystallization sequence: bismuthinite → pavonite → gustavite from sample 1140 (KM72 and this study) the following generalized crystallization sequence is assumed to have taken place in sample 1139: bismuthinite → benjaminite or pavonite → $^{3\cdot41}$Gus$_{116.1}$ continuous to $^{3\cdot83}$Gus$_{79.6}$ → $^{5\cdot90}$L$_{65.7}$ → Ag+Bi-rich galena → Ag+Bi-poor galena.

If no lead is present or if the metal is present only in very small amounts, the sequence might be bismuthinite → benjaminite or pavonite → matildite. This has not yet been recognized in

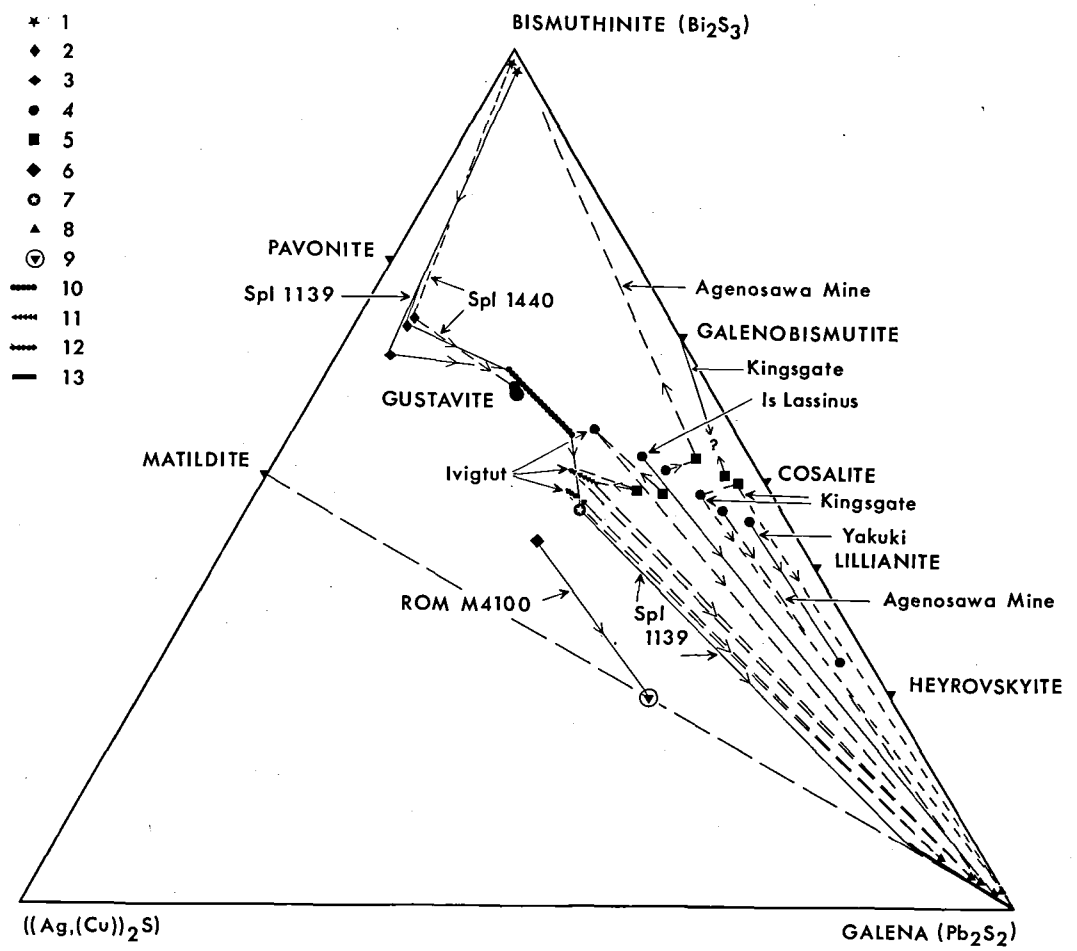

Fig. 10. Diagram showing crystallization trends in natural associations observed during the present study. 1: bismuthinite, 2: pavonite, 3: benjaminite, 4: gustavite-lillianite series members, 5: cosalite, 6: ourayite, 7: $^{5.90}L_{65.7}$, 8: Ag-Bi-galena, 9: decomposed schapbachite; the position of this in the figure is based on the visually estimated proportion between galena and matildite forming the decomposition product. 10: compositional range of gustavite with assumed submicroscopic pavonite in spl. 1139, 11: vikingite compositional range, 12: eskimoite compositional range and 13: compositional range of Ag-Bi-galena in spl. 1139.

naturally occurring materials. Small amounts of copper are contained in all pavonites, benjaminites and bismuthinites examined during the present study. However, the nearly copper-free Agenosawa pavonite (Nedachi et al. 1973) suggests that the above observations also hold when copper is not present.

In the central part of the system (area D, fig. 9) the crystallization sequence is towards galena, (sample 1139). In sample ROM M4100 it is ourayite → schapbachite (now decomposed into galena + matildite).

In the right central part of the system cosalite is a common, characteristic mineral. As pointed out above it is not a member of the LHS. It is also suggested above that its formation has resulted from the presence of small amounts of copper which cannot be accomodated in the structure of the lillianite homologues.

The composition of cosalite varies within narrow, but distinct limits (table 8). When it plots close to or below the cosalite-matildite tie line (fig. 10), e.g. when it has crystallized in mineralizing fluids which are es-

sentially richer in lead than bismuth, the crystallization sequence in silver-poor environments is: cosalite → galena (Kingsgate, Agenosawa), while in more Ag(Cu)-rich environments it appears to be: cosalite→ a lillianite homologue (vikingite and $^{3\cdot74}Gus_{74.9}$ at Ivigtut) → galena. Ontoev (1959) claims the following sequence: lillianite → cosalite-galena solid solution (apparently decomposed heyrovskyite) → cosalite → galena. At Kingsgate (PS 2568, this study) the sequence is cosalite + $^{3\cdot75}Gus_{40.2}$ → galena. In similar silver-poor, but lead-richer environments the crystallization sequence $^{3\cdot86}Gus_{21.0}$ → heyrovskyite ($^{6\cdot68}Hey_{9.6}$) has been recognized in materials from the Yakuki Mine in Japan (this study). When substantial amounts of copper are present, but none or only small amounts of silver, the association cosalite-krupkaite (?) is developed (McElroy Township, Ontario). At Ivigtut significant silver and copper contents have resulted in the following sequences: aikinite + berryite → eskimoite → galena.

In the upper right part of the Ag-Pb-Bi-S system (area C, fig. 9) the sequences have not been resolved. Nedachi et al. (1973) claims the crystallization sequence: bismuthinite → cosalite → phase X ($\approx^{3\cdot94}Gus_{44.0}$) while on materials from the same deposit (Agenosawa Mine) the present study suggests the reverse trend.

Temperatures of formation

Bismuth-bearing sulphides are generally considered to have crystallized in the pneumatolytic and upper hydrothermal ranges, antimony-bearing sulphides in the medium hydrothermal range while arsenic sulphides generally belong to the low hydrothermal to epithermal ranges (e.g. Malakhov 1969). We may therefore except that most of the mineral parageneses belonging to the Ag-(Cu)-Pb-Bi-S system have crystallized at temperatures between 200° and 400°C. Temperatures of formation estimated for some of the materials encountered during the present study are as follows:

Ivigtut, gustavite-cosalite-galena paragenesis: < 300°C (fluid inclusion studies).

Ivigtut, common Ag- and Bi-bearing galena: 400°C–550°C (Karup-Møller & Pauly, in press).

Agenosawa Mine materials: 192°–241°C, (fluid inclusion studies. Nedachi et al. 1973).

Darwin Mine galena mineralizations: above 350°C (homogenization of exsolved minerals in galena. Czamanske & Hall 1975).

Ourayite in spl. ROM M4100: above 215°C. (Stability of schapbachite, KM73b).

Acknowledgements. Interest and assistance of Dr. E. Makovicky, Prof. H. Pauly and cand. real. E. Leonardsen (Copenhagen), Dr. A. Kato (Tokyo), Dr. C. Kieft and Dr. E. A. J. Burke (Amsterdam), Dr. M. Rieder (Prague) and of the institutions who lent their collection specimens are gratefully acknowledged. Dr. J. Bailey has critically read the manuscript. Mrs. A. Eske Christensen assisted at the x-ray research, Mrs. M. Hornstrup typed the text and Mrs. R. Larsen and Mrs. J. Meyer drafted some of the figures. The apparatus used were financed by the grants nos. 511–167–2/69, 511–1887 and 511–3594 from the Danish Natural Science Research Council.

Dansk sammendrag

Følgende nye mineraler hørende til systemet Ag-(Cu)-Pb-Bi-S er fundet ved mikrosonde og røntgenkrystallografiske undersøgelser: vikingit ($Ag_{1.00}$ $Pb_{2.50}$ $Bi_{3.00}$ $S_{7.5}$), eskimoit ($Ag_{1.50}$ $Pb_{3.00}$ $Bi_{3.50}$ S_9), ourayit ($Ag_{12.5}$ Pb_{15} $Bi_{20.5}$ S_{52}) og treasurit ($Ag_{1.75}$ $Pb_{1.50}$ $Bi_{3.75}$ S_8). Flere beslægtede mineralvarieteter er tilstede i så ringe mængde, at røntgenkrystallografisk undersøgelse af disse ikke har været mulig. De er derfor ikke navngivet. Deres sammensætning er bestemt ved mikrosonde. Følgende kendte mineraler er fundet sammenvokset med de nye varieteter og deres sammensætning er ligeledes bestemt med mikrosonde: blyglans, galenobismutit, heyrovskyit, berryit samt varieteter hørende til blandingsrækkerne lillianit-gustavit og vismutglans-aikinit.

De undersøgte mineraler er fundet i parageneser fra forskellige lokaliteter, bl.a. kryolitforekomsten ved Ivigtut i Sydgrønland. De enkelte parageneser er beskrevet, og krystallisationsrækkefølgen indenfor ovennævnte system er diskuteret på grundlag af mineralrelationerne i de enkelte parageneser.

References

Borodaev, Y. S. and Mozgova, N. N. 1971: New group of the sulphbismuthides of Ag, Pb and Cu. *Soc. Min. Geol. Japan, Spec. Issue* 2: 35–41.

Craig, J. R. 1967: Phase relations and mineral assemblages in the Ag-Bi-Pb-S system. *Mineral. Deposita* 1: 278–306.

Czamanske, G. K., and Hall, W. E. 1975: The Ag-Bi-Pb-Sb-S-Se-Te mineralogy of the Darwin lead-silver-zinc deposit, Southern California. *Econ. Geol.* 70: 1092–1110.

Goodell, P. C. 1975: Binary and ternary sulphosalt assemblages in the Cu_2S-Ag_2S-PbS-As_2S_3-Sb_2S_3-Bi_2S_3 system. *Can. Miner.* 13: 27–42.

Graeser, S. 1963: Giessenit – ein neues Pb-Bi-Sulfosaltz aus dem Dolomit des Binnatales. *Schweizer Min. Pet. Mitt.* 43: 471–478.

Harris, D. C. and Chen, T. T. 1975: Gustavite: two Canadian occurrences. *Can. Miner.* 13: 411–414.

Hoda, S. N. and Chang, L. L. 1975: Phase relations in the

systems PbS-Ag_2S-Sb_2S_3 and PbS-Ag_2S-Bi_2S_3. *Am. Miner.* 60: 621–633.

Karup-Møller, S. 1966: Berryite from Greenland. *Can. Miner.* 8: 414–423.

Karup-Møller, S. 1970: Gustavite, a new sulphosalt mineral from Greenland. *Can. Miner.* 10: 173–190.

Karup-Møller, S. 1972: New data on pavonite, gustavite and some related sulphosalt minerals. *N. Jb. Miner. Abh.* 117: 19–38.

Karup-Møller, S. 1973a: A gustavite-cosalite-galena-bearing mineral suite from the cryolite deposit at Ivigtut, South Greenland. *Meddr Grønland 195 (5)*: 1–40.

Karup-Møller, S. 1973b: New data on schirmerite. *Can. Miner.* 11: 952–957.

Karup-Møller, S. 1973c: A giessenite-cosalite-galena-bearing mineral suite from the Björkåsen sulphide deposit at Ofoten in northern Norway. *Norsk geol. Tidsskr.* 53: 41–64.

Karup-Møller, S. 1976: Arcubisite and mineral B – two new minerals from the cryolite deposit at Ivigtut, south Greenland. *Lithos* 9: 253–257.

Karup-Møller, S., and Makovicky, E. 1977: Chemistry and crystallography of pavonite, benjaminite and oversubstituted gustavite. (In prep.)

Karup-Møller, S. and Pauli, H. in press. Galena and associated minerals from the cryolite deposit at Ivigtut, South Greenland. *Meddr Grønland.*

Klomínský, J., Rieder, M., Kieft, C., and Mráz, L. 1971: Heyrovskýite, 6($Pb_{0.86}$ $Bi_{0.08}$ (Ag, $Cu)_{0.04}$ $S.Bi_2S_3$) from Hůrky, Czechoslovakia, a new mineral of genetic interest. *Mineral. Deposita* 6: 133–147.

Kupčík, V., Franc, L., and Makovicky, E. 1969: Mineralogical data on a sulphosalt from the Rhodope Mountains, Bulgaria, *Tschermaks Miner. Petr. Mitt.* 13: 149–156.

Large, R. R. and Mumme, W. G. 1975: Junoite, "wittite", and related seleniferous bismuth sulfosalts from Juno Mine, Northern Territory, Australia: *Econ. Geol.* 70: 369–383.

Lawrence, L. J. and Markham, N. L. 1962: A contribution to the study of the molybdenite pipes of Kingsgate, N. S. W., with special reference to ore mineralogy. *Proc. Aust. Inst. Min. Met.* 203: 67–94.

Leutwein, F. and Hermann, A. G. 1954: Kristallchemische und geochemische Untersuchungen über Vorkommen und Verteilung des Wismuts im Bleiglanz der kiesig-blendigen Formation des Freiberger Gangreviers. *Geologie* 3: 1039–1065.

Makovicky, E. and Karup-Møller, S. 1977a: Chemistry and crystallography of the lillianite homologous series. Part I: Definitions and general properties. *N. Jb. Miner. Abh.* (In press).

Makovicky, E. and Karup-Møller, S., 1977b: Chemistry and crystallography of the lillianite homologous series. Part II: Definition of new minerals: eskimoite, vikingite, ourayite and treasurite. Redefinition of schirmerite and new data on the lillianite-gustavite solid-solution series. *N. Jb. Miner. Abh.* (In press).

Malakhov, A. A. 1969: Bismuth and antimony in galenas as indicators of some conditions of ore formation. *Geochemistry International* 10: 1055–1068.

Mozgova, N. N., Borodaev, Y. S., Syritso, L. E. and Romanov, D. P. (1976): New data on goongarrite (warthaite) and about the identity of heyrovskyite with goongarrite. *N. Jb. Miner. Abh.* 127: 62–83.

Nedachi, M., Takeuchi, T., Yamaoka, K., and Taniguchi, M. (1973): Bi-Ag-Pb-S minerals from Agenosawa mine, Akita Prefecture, Northeastern Japan. *Sci. Rep. Tohoku Univ.* (3) 12: 69–80.

Nuffield, E. W. 1975: Benjaminite – a re-examination of the type material. *Can. Miner.* 13: 394–401.

Ontoev, D. O. (1959): Lillianite from the Bukuka deposit and the conditions of its formation (in Russian). *Dokl. Akad. Nauk. SSSR* 126: 855–858.

Ontoev, D. O., Nissenbaum, P. N. and Organova, N. I. 1960: The nature of high bismuth and silver contents in galena of the Bukukinsk deposit and some problems of isomorphism in the system PbS-Ag_2S-Bi_2S_3. *Geochemistry International* 5: 494–509.

Ontoyev, D. O., Troneva, N. V., Tsepin, A. I., Vyalsov, L. N., and Basova, G. V. 1972: Argentiferous wittite from Eastern Trans-Baikal (In Russian). *Zap. Vsesoyuz. Mineral. Obschtch.* 101: 476–480.

Otto, H. H. and Strunz, H. 1968: Zur Kristallchemie synthetischer Blei-Wismut-Spiessglanze. *N. Jb. Miner. Abh.* 108: 1–19.

Ramdohr, P. 1955: *Die Erzmineralien und ihre Verwachsungen.* Berlin: Akademie. 875 pp.

Salanchi, B. and Moh, G. H. 1969: Die experimentelle Untersuchung des pseudobinären Schnittes des PbS-Bi_2S_3 innerhalb des Pb-Bi-S-Systems in Beziehung zu natürlichen Blei-Wismut-Sulfosalzen. *N. Jb. Miner. Abh.* 112: 63–95.

Srikrishnan, T., and Nowacki, W. 1974: A redetermination of the crystal structure of cosalite, $Pb_2Bi_2S_5$. *Z. Kristallogr.* 140: 114–136.

Syritso, L. F. and Senderova, V. M. 1964: The problem of the existence of lillianite. (In Russian). *Zap. Vsesoyuz. Mineralog. Obshch.* 93: 468–471.

Springer, G., 1967: Die Berechnung von Korrekturen für die quantitative Elektronenstrahl-Mikroanalyse. *Fortsch. Miner.* 45: 103–124.

Van Hook, H. J. 1960: The ternary system Ag_2S-Bi_2S_3-PbS. *Econ. Geol.* 55: 759–788.

Vendrell-Saz, M., Karup-Møller, S. and Lopez-Soler, A. In press. Optical and microhardness study on some Ag-(Cu)-Pb-Bi sulphides. N. Jb. Miner. Abh.